Manuscript Details

Manuscript number	IJRMHM_2019_533_R1
Title	An investigation into the effects of HIP after sintering of WC-ZrC-Co-Cr3C2 cemented carbides
Article type	Research Paper

Abstract

The sintering behaviour of cemented carbides based on WC-ZrC-Co-Cr3C2 powder mixtures have been analyzed by dilatometric and calorimetric methods for different cobalt contents and WC/ZrC ratios. As expected, powder oxide reduction in these compositions is mainly of carbothermic nature. However, depending on the milling conditions, some highly stable Zr-rich oxides are retained in the binder phase after sintering. Hot isostatic pressing (HIP) cycles have been successfully applied for closing residual porosity after vacuum sintering. For a fixed amount of binder phase and a WC/ZrC ratio, the hardness of these materials depends on the amount of residual porosity and WC grain growth control. The best combination of hardness and toughness is found for alloys with 8 wt.%Co and WC/ZrC wt. ratios of 6.46. HIP treatments induce the formation of a compact and well adhered layer mainly comprised of Zr oxides and WC grains. The cobalt binder phase migrates from this layer towards the sample bulk likely due to the loss of wettability on these Zr rich oxides. Hot hardness is higher for the alloy with higher WC/ZrC ratio suggesting that this property depends on both the volume fraction of (ZrxW1-x)C and WC phases and their degree of contiguity.

Keywords	Cemented carbides, WC, ZrC HIP after sintering, hot hardness

Corresponding Author	Jose M. Sanchez
Corresponding Author's Institution	CEIT-IK4
Order of Authors	Tomas Soria Biurrun, Belen Lopez-Ezquerra, Lorena Lozada, Steven Moseley, Patricia Alveen, Marc Elsen, Andrea Müller-Grunz, Michael Magin, Ralph Useldinger, Jose M. Sanchez

Submission Files Included in this PDF

File Name [File Type]

Cover letter.doc [Cover Letter]

answer to referee comments.docx [Response to Reviewers]

HIGHLIGHTS.docx [Highlights]

MANUSCRIPT_WC-ZrC-CoCr_revised.doc [Manuscript File]

Fig. 1a.ppt [Figure]

Fig. 1b.ppt [Figure]

Fig. 2a.ppt [Figure]

Fig. 2b.ppt [Figure]

Fig. 2c.ppt [Figure]

Fig. 3a.ppt [Figure]

Fig. 3b.ppt [Figure]

Fig. 4.ppt [Figure]

Fig. 5.ppt [Figure]

Fig. 6.ppt [Figure]

Fig. 7.ppt [Figure]

Fig. 8a.ppt [Figure]

Fig. 8b.ppt [Figure]

Fig. 8c.ppt [Figure]

Fig. 9.ppt [Figure]

Fig. 10.ppt [Figure]

Fig. 11.ppt [Figure]

Table 1.docx [Table]

Table 2.docx [Table]

Table 3.docx [Table]

Table 4.docx [Table]

Table 5.docx [Table]

Table 6.docx [Table]

Table 7.docx [Table]

declaration-of-competing-interests.docx [Conflict of Interest]

Author statement.docx [Author Statement]

To view all the submission files, including those not included in the PDF, click on the manuscript title on your EVISE Homepage, then click 'Download zip file'.

Research Data Related to this Submission

There are no linked research data sets for this submission. The following reason is given:
Data will be made available on request

July, 16th, 2019

Dear Editor:

We would like to submit the article entitled “An investigation into the effects of HIP after sintering of WC-ZrC-Co-Cr_3C_2 cemented carbides” for publication in International Journal of Refractory Metals and Hard Materials. Please, do not hesitate to contact us if you have any questions.

Yours sincerely,

J.M. Sánchez

CEIT-IK4 . Paseo Manuel de Lardizabal, 15, 20018, San Sebastián, Spain.

phone: 34-943-212800
fax:34-943-213076
email: jmsanchez@ceit.es

Ref: IJRMHM_2019_533
Title: An investigation into the effects of HIP after sintering of WC-ZrC-Co-Cr3C2 cemented carbides
Journal: International Journal of Refractory Metals and Hard Materials

Answers to Reviewer 1 comments:

1- Its not possible to review this manuscript because Figures are missing!

Answer:
We are sorry. The missing figures were included as xlsx files. During first submission, we received confirmation from EVISE software that uploading had been successful. Anyhow, we have included these figures in a new format that has been uploaded again in the revision process.

2- Furthermore the experimental procedure is curious. Three samples with rather different composition? Comparison of the results is not possible.

Answer:
We don't agree with this comment. Alloys 1 and 2 were designed to study the effect of different Co contents on sintering and mechanical properties but keeping constant the WC/ZrC and the Cr/Co ratios. Alloy 2 and 3 have the same Co and Cr content but different amount of ZrC. These are the comparisons analyzed in the text.

3- The HIP after sintering failed and ZrO2 was formed. The detailed characterization of the failed samples should not be the topic of a manuscript.

Answer:
Again, we do not agree with the reviewer comment. In our opinion, HIP did not fail. These cemented carbides were produced with very high ZrC contents (this is the main novelty of this work) and we observed that are not easy to obtain in fully dense form. Firstly, we used vacuum sintering experiments and the materials with closed porosity state were submitted to HIP cycles. In Alloy 3, density obtained after HIPing was higher than that obtained after vacuum sintering. Therefore, we consider that the HIP cycle was successful. Our data also show that HIP conditions (1450°C-150MPa-1 h) are not enough to remove residual porosity in Alloy 2. This is also a relevant result that shows that sinterability decreases with the ZrC content.

The idea of using such high ZrC contents in the beginning was to evaluate their behavior under these processing routes. The surface layers obtained with high ZrO2 content are completely different from oxide layers generated by heating in air. We have analyzed such oxide layers in other materials (see for instance [Aristizabal et al. IJRM&HM 2010*]) and these are highly porous in comparison with those obtained in this work. Therefore, we consider that including the study of these layers in the work is relevant and meaningful.

*M. Aristizabal, N. Rodriguez, F. Ibarreta and R. Martinez, J.M. Sanchez. "Liquid phase sintering and oxidation resistance of WC-Ni-Co-Cr cemented carbides" International Journal of Refractory Metals and Hard Materials, 28, (2010), 516-522.

Answers to Reviewer 2 comments:

1- **In section 3.2: Authors mention that elimination of residual porosity is more difficult as Co and WC decreases. Is this true? Would not be dependent on the addition of ZrC? Later they mention the good wetting of WC by Co and this would not change on Co/WC, as expected for WC-Co grades, regardless the amount of each phase.**

Answer:

The referee comment is completely true. The sentence is misleading. What we wanted to mean is that densification is more difficult as the Co content and WC/ZrC ratio decrease. We have changed the previous sentence by this one and marked it in blue (page 4).

2- **In section 3.2: Include in Figure 7 the explanation of each symbol and ICDD number of each patter from which the peaks were classified.**

Answer:

We had already included this information in the Figure caption, but we agree that is clearer to have it included in the figure itself. This has been corrected in the revised version.

3- **Section 3.3: At the beginning of paragraph 3, the authors mention ZrC/WC ratio. It would better to say WC/ZrC as it is mentioned along the text and in Table 1, to avoid confusion.**

Answer:
The change suggested has been included in the revised version.

4- **Section 3.3: The authors mention that diffusion of Zr atoms is activated by a higher volume fraction of liquid. Diffusion is a process that depend only on diffusion coefficient, activation energy and temperature, not on the amount of liquid. Please revise.**

Answer:

We appreciate the reviewer comment and agree with it. More experiments should be carried out in order to understand this phenomenon. We have removed the mentioned sentence (in line 17 or page 6) and we think that the text does not lose coherency.

5- **Section 3.3: Could the authors explain why Co content on the top layer is similar for the 3 compositions? An explanation of migration of Co inwards is given but not an explanation on the amount of Co found, especially when comparing Alloy 1 with Alloys 2 and 3.**

Answer:

This is likely due to the good wetting behavior between Co and WC. As there are still some WC grains in the outer layer it is possible that the cobalt that remains in this oxide layer is the one

in contact with WC grains. We are now carrying out other experiments (thermal shock tests) and we'll investigate this possibility in deeper detail.

6- Conclusions: "The best combination of hardness…is found for alloys with…WC/ZrC wt. ratio of 6.46." It would be better to say 6.50, consistently with Table 1.

Answer:

This has been changed in the revised version according to the reviewer suggestion.

HIGHLIGHTS

An investigation into the effects of HIP after sintering of WC-ZrC-Co-Cr_3C2 cemented carbides

1- Liquid phase sintering of WC-ZrC-Co-Cr_3C_2 powder mixtures has been investigated for different cobalt contents and ZrC/WC ratios.

2- Residual porosity increases in these materials for low Co and high ZrC contents.

3- Zr-rich oxides are retained in the metallic binder phase after vacuum sintering when using high energetic milling conditions.

4- The role of ZrC as WC grain growth inhibitor has been confirmed by analyzing the evolution of hardness after HIP treatments

5- The best combination of hardness and toughness is found for alloys with 8 wt.%Co and WC/ZrC wt. ratios of 6.46.

6- HIP treatments applied to vacuum sintered specimens induce the formation of oxide rich surface layers. These consists of a mixture of tetragonal and monoclinic zirconia and tungsten carbide grains. Cobalt migrates from this layer towards the sample bulk likely due to the loss of wettability on these Zr rich oxides.

An investigation into the effects of HIP after sintering of WC-ZrC-Co-Cr_3C_2 cemented carbides

Tomas Soria[1,2] tsoria@ceit.es; Belen Lopez[3] belen_1988@hotmail.com; Lorena Lozada[1,2] llozada@ceit.es;Steven Moseley[3] steven.moseley@hilti.com; Patricia Alveen[3] patricia.alveen@hilti.com; Marc Elsen[4] elsen.marc@education.lu; Andrea Müller-Grunz[4] andrea.mueller@ceratizit.com; Michael Magin[4] Michael.Magin@ceratizit.com; Ralph Useldinger[4] Ralph.Useldinger@ceratizit.com; Jose M. Sánchez[1,2] jmsanchez@ceit.es

1- CEIT-IK4, Manuel Lardizabal 15, 20018 Donostia / San Sebastián, Spain.

2- UNIVERSIDAD DE NAVARRA, Tecnun, Manuel Lardizabal 13, 20018 Donostia / San Sebastián, Spain.

3- HILTI CORPORATION, Feldkircherstrasse 100, LI-9494 Schaan, Liechtenstein

4- CERATIZIT, Luxembourg S.à r.l., Mamer, Luxembourg

Abstract

The sintering behaviour of cemented carbides based on WC-ZrC-Co-Cr_3C_2 powder mixtures have been analyzed by dilatometric and calorimetric methods for different cobalt contents and WC/ZrC ratios. As expected, powder oxide reduction in these compositions is mainly of carbothermic nature. However, depending on the milling conditions, some highly stable Zr-rich oxides are retained in the binder phase after sintering. Hot isostatic pressing (HIP) cycles have been successfully applied for closing residual porosity after vacuum sintering. For a fixed amount of binder phase and a WC/ZrC ratio, the hardness of these materials depends on the amount of residual porosity and WC grain growth control. The best combination of hardness and toughness is found for alloys with 8 wt.%Co and WC/ZrC wt. ratios of 6.46. HIP treatments induce the formation of a compact and well adhered layer mainly comprised of Zr oxides and WC grains. The cobalt binder phase migrates from this layer towards the sample bulk likely due to the loss of wettability on these Zr rich oxides. Hot hardness is higher for the alloy with higher WC/ZrC ratio suggesting that this property depends on both the volume fraction of $(Zr_xW_{1-x})C$ and WC phases and their degree of contiguity.

1. Introduction

Hot hardness and oxidation-corrosion resistance are key properties for the performance of hardmetal tools at high temperatures [1,2]. The “so-called” P and M hardmetal grades are a good example of such materials [3]. Specifically designed for high speed machining of steel, these ceramic-metal composites exhibit excellent crater wear resistance due to the combination of WC grains and γ phases (comprised of (M,W)C solid solutions of carbides with M = Ti, Ta, Nb) both embedded in the metallic Co binder. These γ-type carbides have higher contiguity than WC grains and withstand higher loads at high temperatures in comparison with WC-Co alloys. In addition, their solubility in steel at the temperatures generated during cutting is also much lower than that of WC-Co materials [2]. It is well known that TiC, TaC, NbC additions inhibit WC grain growth during sintering [4] and that the aforementioned (M,W)C γ phases precipitate upon cooling from the liquid phase [5,6]. However, information is still lacking for certain combinations like those including zirconium carbide and chromiun carbide additions to the WC-Co system [7-9]. These two carbides present very different solubilities both in tungsten carbide and cobalt. Moreover, zirconium has very high affinity for oxygen, which could have significant influence in the solid-gas reactions occurring during sintering. In this work, different WC-ZrC-Co-Cr_3C_2 powder mixtures have been processed by HIP after sintering in order to analyze their shrinkage behaviour and characterize their microstructural evolution during liquid phase sintering.

2. Experimental procedure

The compositions of the powder mixtures used in these experiments are included in Table 1. As observed, Alloys 1 and 2 have different Co contents but the same WC/ZrC ratio. On the other hand, Alloys 2 and 3 have the same Co content but different WC/ZrC ratios. Cr_3C_2 additions are calculated to be 7% of the cobalt content in all compositions. Mixing/milling was carried out in a planetary equipment at 100 rpm for 5 hours using hexane as liquid media and a ball to powder weight ratio of 6 to 1. Alloy 1 was milled at 200 rpm. However, rotation speed was reduced down to 100 rpm for Alloys 2 and 3. This was decided after checking oxygen contents of green compacts. Paraffin, used as pressing aid, was added during the last milling hour. Two paraffin contents were used depending on the amount of metallic addition: 0.7 wt.% for samples with 24 wt.%Co and 1.9 for those with 8 wt.%Co. A higher paraffin content is needed in the sample with lower metal content due to its poorer compactability. After milling, the powders were dried for 1 h. at atmospheric pressure in a thermostatic bath (90+/-2ºC). Green compacts were obtained by double action pressing at 160 MPa. The

sinterability of the different powder mixtures was analysed by calorimetry, thermogravimetry (TGA/DSC Setaram Setsys Evolution 16/18) and dilatometry (Netzsch TA 402 E/7). These experiments were carried out on cylinders (5 mm high and ϕ 5 mm) using a heating rate of 10ºC/min up to 1450ºC. Dwelling time at this temperature was 1 hour for dilatometric experiments and 5 min. for DSC/TGA tests (both types of experiments were made in Ar atmosphere, 1 bar). The onset of DSC and shrinkage rate peaks were determined by using the SETSOFT software [10]. Vacuum sintering experiments (VS) were carried out in a industrial furnace with graphite heating elements and chamber at 10ºC/min up to 1400ºC. The vacuum level used during this step was 10^{-2} mbar. Above this temperature, the pressure was increased up to 100 mbar by injecting argon in the furnace chamber and maintained during the 1 h sintering plateau. Hot isostatic pressing was also applied to a selected group of sintered specimens in order to eliminate all residual porosity. In these cycles, a temperature of 1400ºC and an isostatic pressure of 150 MPa were simultaneously applied to the previously sintered samples for 1 hour using Ar gas as pressing fluid. C and O contents were measured by means of infrared spectrometry both in green compacts and sintered materials. Standard ISO 3369 was used for density measurements. The sintered specimens were ground and polished down to 1 µm diamond paste for microstructural analysis, which was carried out by optical microscopy, scanning electron microscopy (FEG-SEM) and energy dispersive X-ray spectroscopy (EDS). Phase identification was carried out by X-Ray diffraction (XRD) (with Ni-filtered CuKα radiation) using Bragg-Brentano configuration and lattice parameters where calculated by using the Nelson Riley function [11]. Mechanical characterization included the measurement of hardness (ISO 3878) and the estimation of fracture toughness from indentation cracks [12]. Finally, hot hardness tests were carried out under vacuum (10^{-3} mbar). Polished samples were heated at 10ºC/min up to the different testing temperatures: 500ºC, 600ºC and 700ºC. The maximum applied load was 10 kg and was kept for 15 s before unloading.

3. Results and discussion

3.1. Thermal analyses: Dilatometry, Calorimetry and Thermogravimetry.

Dilatometric curves show certain swelling in all three compositions during the heating ramp up to 950-1000ºC (Fig. 1a). This occurs because thermal expansion of the compacts dominates over solid phase sintering phenomena in this temperature range. The highest swelling corresponds to the material with

higher metal content (Alloy 1), since the thermal expansion coefficient of cobalt is 2.5 and 1.9 times higher than that of WC or ZrC respectively [2,13]. Temperatures corresponding to the first shrinkage rate peak are very similar for the three compositions (between 1228 and 1238ºC) (Fig. 1b and Table 2) and the highest shrinkage rate corresponds to the alloy with higher metal content (Alloy 1). These results confirm that the shrinkage rate of WC-ZrC-Co-Cr_3C_2 alloys is reduced as the metal content and the WC/ZrC ratio decrease. Both solid and liquid phase sintering mechanisms are involved in mass transport during the heating ramp of the sintering cycle.

DSC experiments confirm that the shrinkage onset occurs 27-30ºC below melting onsets in alloys with higher ZrC contents (i.e. Alloys 1 and 2) (Fig. 2). This diffference is reduced to just 13ºC for Alloy 3 (with much lower ZrC content). As expected, the amount of liquid, proportional to the area above DSC peaks, is 2.7 times higher for Alloy 1 than for Alloy 2 or Alloy 3. It is generally agreed that shrinkage is dominated by rearrangement of solid particles due to capillary forces induced by liquid spreading through the compact structure [14]. In this case, it is obvious that a higher amount of liquid enhances this process inducing a high shrinkage acceleration. On the other hand, for Alloys 2 and 3, both with similar amounts of liquid phase, the differences in shrinkage could be explained by the different wetting behaviour of liquid cobalt on WC or ZrC grains (with wetting angles of 0º and 36º respectively)[15]. In the sintering plateau (1 hour at 1450ºC), the shrinkage behaviour is also different. Alloy 2 has 3% shrinkage whereas Alloys 1 and 3 have only 1.9%. This could be explained by considering that solution reprecipitation mechanisms, involved in the formation of the (Zr_x, W_{1-x})C phase, are active in removing residual porosity at high temperatures in the presence of a liquid phase. Finally, the total linear shrinkage of Alloy 1 (with 31.5 vol.% of metal) is 20% higher than those of Alloys 2 and 3, which are very similar between them. This corroborates that final shrinkage after sintering is strongly affected by the amount of liquid during sintering and not much by the WC/ZrC ratio within the studied compositional range. The highest mass losses measured by TGA occur between 200ºC and 400ºC and correspond to the organic binder burnout (Fig. 3a). These mass losses are higher for Alloy 3 due to its higher paraffin content, this higher amount of paraffin was required to avoid the presence of cracks after pressing. Above 400ºC, differences in degassing activities are better observed by differentiating TGA curves with respect to time (Fig. 3b).

In both cases, significant mass losses are detected between 1170ºC and 1250ºC, which, according to the information provided by Ellingham diagrams [16], coincides with the temperatures required for the carbothermal reduction of Cr_2O_3 (Fig. 4). Some authors associate these outgassing phenomena with

the dissolution of Cr_3C_2 carbide in solid cobalt, which also occurs in this temperature range [17]. As this chromium carbide is dissolved in solid cobalt, free carbon is released and is, therefore, available for reaction with chromium oxides. At intermediate temperatures, between 400ºC and 1170ºC, mass losses are very low, although slightly higher for Alloy 3 (with lower metal and higher WC contents). This is consistent with the previous explanation, since the solubility of WC in cobalt is 6 times higher than that of ZrC [18,19].

3.2. Vacuum sintering experiments

Data included in Table 3 confirm that the alloy with higher Co content (Alloy 1) is close to full density after vacuum sintering at 1400ºC for 1 hour. However, the other two alloys (with lower Co content) require a higher sintering temperature (1475ºC) to reach similar density levels. This is in good agreement with data obtained from dilatometric experiments, although the latter were carried out in argon. The increase in density obtained by rising the sintering temperature from 1400ºC to 1475ºC is higher for Alloy 3 than for Alloy 2, that is, for the alloy with higher WC/ZrC ratio.

Both results prove that the elimination of the last residual porosity in WC-ZrC-Co-Cr_3C_2 alloys is more difficult as their Co content and the WC/ZrC ratio decrease. As described above, this is related to the better wetting of WC grains by liquid cobalt and also to the higher solubility of WC phase in this liquid phase, both compared to those of the $(Zr_x, W_{1-x})C$ phase.

C and O contents of green compacts and sintered specimens are included in Table 4. The oxygen content of Alloy 1 is 60% higher than those of Alloys 2 and 3. This confirms that oxidation during milling can be reduced by reducing the milling rotation speed from 200 to 100 rpm. After sintering, the amount of oxygen removed from the samples is similar for the three compositions (around 0.4 wt.%). This leaves an oxygen content 4 times higher for Alloy 1 than for the other two. On the other hand, carbon contents measured after sintering are close to those calculated from the stoichiometry of the carbides used in the powder mixtures (excluding that of the paraffin). Assuming that approximately 0.3 wt.% C is lost to the carbothermal reduction of powder oxides, there should be other carbon sources available to explain the final C contents measured in the sintered specimens. These could be, for example, the residues of paraffin pyrolysis or the C provided by the slight decomposition of the heating elements and the furnace crucible, both made of graphite. SEM images of sintered specimens of Alloy 1 show the presence of free C (dark flakes pointed by the blue arrow in Fig. 5) along with zirconium

oxide precipitates embedded in the metallic binder phase (pointed by the black arrow in Fig. 5). Although EDS analyses have not enough spatial resolution for a quantitative analysis of such oxides, qualitative estimation of their Zr/O ratio is compatible with that of ZrO_2. These oxides remain in the microstructure after sintering because their carbothermal reduction requires much higher temperatures (Table 4). Such oxides have not been found in Alloys 2 and 3 (Fig. 6), which is clearly related to their their lower nominal oxygen content after milling.

Apart from this, carbon and oxygen contents of these two compositions show that decarburization is higher for the alloy with higher WC/ZrC ratio. This is consistent with the higher mass losses found in this material during the heating ramp between 400ºC and 1200ºC and, as previously described, proves that the carbothermal reduction of powder oxides is enhanced by the higher solubility of WC in the metallic binder phase compared to that of ZrC.

Main crystalline phases identified by X-ray diffraction are hexagonal WC carbide, $(Zr_x, W_{1-x})C$ mixed carbide and Co-FCC phase. The lattice parameters calculated for the two latter phases are included in Table 5 [11] (Fig. 7). As expected, the lattice parameter corresponding to the metallic binder is higher than that of pure cobalt and confirms the presence of larger atoms in solid solution (i.e. W, Cr or both). No Zr was found in EDS analyses corresponding to the binder phase (see Fig. 5). As $(Zr_x,W_{1-x})C$ mixed carbides are concerned, their lattice parameters are close to those found in ICDD PDF-4 database for Zr/W= 4. These lattice parameters decrease by increasing the sintering temperature or by increasing the WC/ZrC ratio suggesting that, under such conditions, $x < 0.8$.

3.3. HIP after sintering

As described in the previous section, porosity levels are unacceptable for the alloys with lower Co content. The effect of HIP treatments on the removal of this residual porosity is included in Table 3.

These data confirm that both the WC/ZrC ratio and the residual porosity left after vacuum sintering have an important effect on the density achieved after HIPing. Thus, specimens of Alloy 2 with 96.5% theoretical density (T.D.) after VS had no additional densification after HIPing. However, those with 98.3% T.D. increased this value up to 98.8%. T.D. after the same HIP cycle (from 12.44 to 12.51 g/cm^3).

For Alloy 3 (with higher WC/ZrC ratio), densification achieved after VS at 1475ºC is already above 99%T.D. Therefore, the potential increase in density produced by HIP is below the resolution limit of the measurement technique (ISO-3369). On the other hand, when HIP is applied to Alloy 3 specimens with 96.2%T.D., densification is more efficient than in the case of Alloy 2.This corroborates that the wetting properties of the liquid are very important in order to remove residual porosity in the range of 4-5 vol.%.

IR espectrocopy analyses show that, whereas carbon contents are not significantly modified by the HIP treatment, those of oxygen increase significantly (Table 4).There are two possible reasons for this behavior. Firstly, vacuum levels during the heating ramp of the HIP cycle are not as high as those achieved in vacuum sintering experiments (10^{-1} mbar vs. 2.10^{-2} mbar). Moreover, although the oxygen content in the argon gas used for pressurizing the HIP vessel is only 2 ppm, oxygen activity is multiplied by 1500 at the maximum pressure level of the HIP cycle. SEM images taken from these specimens confirm the presence of surface layers with high oxygen content (Fig. 8).

These layers, with thicknesses that range from 80 to 100 μm, are very different from those reported for hardmetals oxidized in atmospheric conditions since they are fully dense and well adhered to the substrate. Their main constituents are Zr rich oxides and WC grains. The layer formed at the surface of Alloy 1 has higher Zr content than those of Alloys 2 and 3 (Table 6). The driving force for this phenomenon would be the presence of a certain oxygen activity in the chamber of the HIP furnace. It is also worth noting that cobalt migrates from the sample surface to its interior. Cobalt content in the oxidized layers is very similar for the 3 compositions, which suggests that is not related to the initial cobalt content of the alloys. A possible explanation would be that the wettability of the Co-rich liquid phase onto Zr-rich oxides is poor, forcing the inward cobalt migration by capillarity forces far from the region with high concentration of Zr-rich oxides. Crystallographic phases, identified in these oxidized layers by glancing angle incidence XRD, include hexagonal WC, $(Zr_x, W_{1-x})C$ and both monoclinic and tetragonal zirconia (Fig. 9). The ratio between these two ZrO_2 phases has been estimated by the quotient of the areas under their most intense peaks: (101) for the tetragonal phase (-111) for the monoclinic one (see 00-037-1484 and 01-070-7358 ICDD reference patterns). $I_{MONOCLINIC\ (-111)}/I_{TETRAGONAL\ (101)}$ ratios are equal to 4.18 for Alloy 1, 4.17 for Alloy 2 and 3.00 for Alloy 3 (all processed by HIP + VS at 1400ºC-1h). This suggests that the monoclinic phase is dominant in all cases, although the fraction of tetragonal zirconia increases with the WC/ZrC ratio. The formation of

these oxide layers could have an impact of the oxidation and corrosion resistance of these alloys. Additional research is in progress in order to investigate their potential passivation effect. On the other hand, the presence of tetragonal zirconia as a constituent of these surface layers could also hinder crack growth by strain-induced transformation, similarly to that observed in other tetragonal zirconia containing systems [20].

Hardness values of vacuum sintered specimens with and without HIP treatment are included in Table 7.

These data correspond to the sample bulk, far from the oxide layers described above. Results are clearly related to the amount of residual porosity left in the samples and their grain growth kinetics. Thus, a significant hardening is obtained in Alloy 2 by increasing the sintering temperature from 1400ºC to 1475ºC. In this case, the elimination of residual porosity dominates over WC grain growth (Table 3). However, in Alloy 3 (with a higher WC/ZrC ratio), hardness values are very similar for both sintering temperatures. This could be explained by considering that the increase in hardness expected from a similar densification effect is compensated by a higher WC grain growth (Tables 3 and 7). Therefore, this corroborates the WC grain growth inhibition effect of ZrC additions in these alloys. HIP after sintering treatments confirm these phenomena since hardness is maintained or even increased in Alloy 2 and dramatically decreased in Alloy 3. Porosity is completely eliminated in both alloys by applying 150 MPa and 1400ºC for 1 hour. Therefore, the softening observed in Alloy 3 is due to the loss of control over WC grain growth.

Plotting hardness vs. K_{1c} values obtained by indentation (Fig. 10), it is confirmed that two materials (Alloy 2 sintered at 1475ºC-1h and Alloy 3 obtained by VS at 1475ºC-1h + HIP) exhibit values within the range of those obtained with commercial products based on WC-6 wt. %Co (10 vol.%) with different WC mean grain sizes. As previously described, hardness is better retained in Alloy 2 due to its higher ZrC content.

Samples with best combination of hardness and toughness at room temperature were selected for hot hardness experiments (Fig. 11). Hardness loss from 20ºC to 700ºC is 47% for Alloy 2, 49% for Alloy 3 and 51% for the WC-Co reference. This confirms that the presence of $(Zr_xW_{1-x})C$ mixed carbides increases hot hardness, similarly to that reported for other γ phases (i.e. $((Ti,Ta,Nb)_xW_{1-x})C$) [2]. It is worth mentioning that, between room temperature and 600ºC, hardness is slightly higher for the material with higher WC/ZrC ratio (i.e. the material with higher volume fraction of WC grains). This

indicates that the intrinsic hot hardness of $(Zr_xW_{1-x})C$ cubic carbides is not as high as that of tungsten carbide. However, according to these results, there should be a certain optimum volume fraction of $(Zr_xW_{1-x})C$ cubic carbides at which contiguity effects provide higher rigidity at high temperatures.

3 Conclusions

Densification of WC-ZrC-Co-Cr_3C_2 powder mixtures by liquid phase sintering is enhanced by increasing the amount of liquid phase and the sintering temperature. However, for low WC/ZrC ratios, unacceptable porosity levels are found after conventional vacuum sintering. C and O losses measured by IR spectrometry confirm that the reduction of powder oxides is mainly of carbothermic nature. However, highly stable Zr-rich oxides, likely produced during milling, remain embedded in the binder phase after sintering. For a fixed amount of binder phase and WC/ZrC ratio, the hardness of these materials depends on the amount of residual porosity and WC grain growth control. The best combination of hardness and toughness is found for alloys with 8 wt.%Co and WC/ZrC wt. ratio of 6.50. Hot isostatic pressing cycles used for closing residual porosity after vacuum sintering generate surface layers with thickness ranging from 60 to 200 microns comprised of zirconia and tungsten carbide grains. An inward migration of the Co-rich binder phase is detected in all cases. This is likely due to the loss of wettability on zirconia grains. These layers are dense and well adhered to the material bulk. XRD analyses confirm that both tetragonal and monoclinic zirconia are found in these surface layers. Tetragonal to monoclinic ratio has been found to increase with that of WC to ZrC. The highest hot hardness corresponds to the alloy with 8 wt.%Co and a WC/ZrC ratio of 17.3, being 11% higher at 500ºC than that corresponding to a commercial WC-6wt.% Co reference with the same mean WC grain size.

Acknowledgments

HILTI CORPORATION and CERATIZIT GROUP are gratefully acknowledged for the financial support of this work. Special thanks to Dr. J. Pötsche (IKTS-Fraunhofer) for carrying out hot hardness experiments.

References

1- Exner HE. Physical and chemical nature of cemented carbides. Int Met Rev 1979; 4:149–73.

2- Gurland J., “New scientific approaches to development of tool materials,” Int. Mater. Rev. 1988;

33, 1: 151–166.

3- ISO 513:2012 Classification and application of hard cutting materials for metal removal with defined cutting edges -- Designation of the main groups and groups of application.

4- Hayashi K, Fuke Y, Suzuki H, ‘‘Effects of addition carbides on the grain size of WC–Co alloy,’’ J. Jpn. Soc. Powder Met.1972; 19 [2]: 67–71.

5- Markström A, Frisk K, Sundman B, ‘‘A revised thermodynamic description of the Co–W–C system,’’ J. Phase Equilib. Diffus. 2005; 26: 152–60.

6- Frisk K, Markström A, ‘‘Effect of Cr and V on phase equilibria in WC–Co based hardmetals,’’ Int. J. Mater. Res., 2008; 99: 287–93.

7- Weidow J, Zackrisson J, Jansson B, Andren HO, “Characterisation of WC-Co with cubic carbide additions,” Int. J. Refract. Met. Hard Mater. 2009, 27: 244–248.

8- Weidow J, Andren HO, “Grain and phase boundary segregation in WC-Co with TiC, ZrC, NbC or TaC additions,” Int. J. Refract. Met. Hard Mater. 2011; 29; 1: 38–43.

9- Weidow J, Johansson S, Andrén HO, Wahnström G, “Transition metal solubilities in WC in cemented carbide materials”, J. Am. Ceram. Soc. 2011; 94 [2]: 605–610.

10- SETARAM Instrumentation. Setsys evolution 16/18. SETSOFT user manual, (2002), 39.

11- Nelson JB, Riley DP, An experimental investigation of extrapolation methods in the derivation of accurate unit-cell dimensions in crystals, Proc. Phys. Soc. 1945; 57: 160-177.

12- Shetty K, Wright IG, Mincer PN, Clauer AH, “Indentation fracture of WC-Co cermets”, J. Mat. Sci. 1977; 20: 1873-1882.

13- Touloukian YS, Thermophysical Properties of Matter, Vol. 12, Thermal Expansion, IFI/Plenum, New York, 1975.

14- German RM, Powder Metallurgy Science, MPIF, 1997, 2ND Ed Princeton, N Jersey 08540-6692 USA: 274-281.

15- Eustathopoulos, N. Wetting properties of metal/non oxide ceramic systems, “ in Wettability at High Temperatures, Amsterdam, New York, Pergamon, 1999: 261–316

16- Alloy Phase Diagrams, ASM Handbook, vol. 3, ASM International, Materials Park, Ohio, 1992.

17- Wang H, Webb T, Bitler JW, "Different effects of Cr_3C_2 and VC on the sintering behavior of WC-Co materials, Int. J. Refract. Met. Hard Mater. 2015; 53: 117-122.

18- Ettmayer, P, Kolaska, H, Lengauer, W, Dreyer, K; Ti(C,N) cermets — Metallurgy and properties. Int. J. Refract. Met. Hard Mater.; 1995; 13: 343–351.

19- Upadhyaya GS, Materials science of cemented carbides- an overview, Mater. Design 2001; 22: 483-489

20- Claussen N, "Fracture toughness of Al_2O_3 with and unstabilized ZrO_2 dispersed phase", J.Am. Ceram. Soc, 1976; 59, 1-2:49-51.

FIGURE CAPTIONS

Fig. 1 (a) Shrinkage and (b) shrinkage rate corresponding to WC-ZrC-Co-Cr_3C_2 alloys included in Table 1.

Fig. 2 Comparison between shrinkage rate and DSC heat flow peaks corresponding to WC-ZrC-Co-Cr_3C_2 compositions: (a) Alloy 1, (b) Alloy 2, and (c) Alloy 3.

Fig. 3 (a) TGA plots obtained during the heating ramp used in DSC experiments of WC-ZrC-Co-Cr_3C_2 alloys, (b) mass loss rates obtained by differentiating these TGA curves with respect to time.

Fig. 4 Ellingham diagram showing theoretical temperatures required for reduction of several oxides present in the powder mixtures (Thermocalc® SSUB4).

Fig. 5 BSE-SEM image corresponding to Alloy 1 obtained by VS at 1400ºC-1h. EDS analyses corresponding to free C, Co-Cr rich metallic binder phase, $(Zr_xW_{1-x})C$ phase and Zr-rich oxides are also included.

Fig. 6 SE-SEM images corresponding to: (a) Alloy 2 obtained by VS at 1400ºC-1h, (b) Alloy 3 - VS@1400ºC-1h, (c) Alloy 2 - VS at 1475ºC-1h and (d) Alloy 3 - VS at 1475ºC-1h

Fig. 7 XRD patterns corresponding to WC-ZrC-Co-Cr_3C_2 alloys after vacuum sintering at 1400ºC for 1 h: (a) Alloy 1, (b) Alloy 2 and (c) Alloy 3. ICDD PDF-4 database reference codes included. (▼) Tungsten carbide WC (01-089-2727) , (○) FCC-Cobalt (01-089-4307) and (☒) Tungsten zirconium carbide. $(Zr_xW_{1-x})C$ (01-071-6325, for x=0.8).

Fig. 8 BSE-SEM micrograph of WC-ZrC-Co-Cr_3C_2 alloys obtained by VS at 1400ºC-1h + HIP a 1400ºC-150MPa-1h: (a) Alloy 1, (b) Alloy 2 and (c) Alloy 3. EDS mappings of the corresponding elements are included in each case.

Fig. 9 XRD diffraction patterns obtained by the glancing angle technique (ω = 3º) from the surface of WC-ZrC-Co-Cr_3C_2 alloys after VS @ 1457ºC for 1 h + HIP treatment. ICDD PDF-4 database reference codes included. (▼) Tungsten carbide WC (01-089-2727), (☒) Tungsten zirconium carbide (Zr_xW_{1-x})C (01-071-6325, for x=0.8), (T) tetragonal zirconia (01-070-7358) and (m) monoclinic zirconia (00-037-1484).

Fig. 10. Hardness (HV10) vs. K_{1c} (obtained by indentation) of WC-ZrC-Co-Cr_3C_2 alloys obtained by different consolidation routes. Values corresponding to two commercial WC-6wt.%Co grades (with medium and coarse WC grain size) are also included.

Fig. 11. Hardness (HV10) as a function of temperature for Alloy 2 (VS @ 1475ºC-1h+HIP) and Alloy 3 (VS @ 1475ºC-1h). Data of WC-10vol.%Co (medium WC grain size) are also included as a reference.

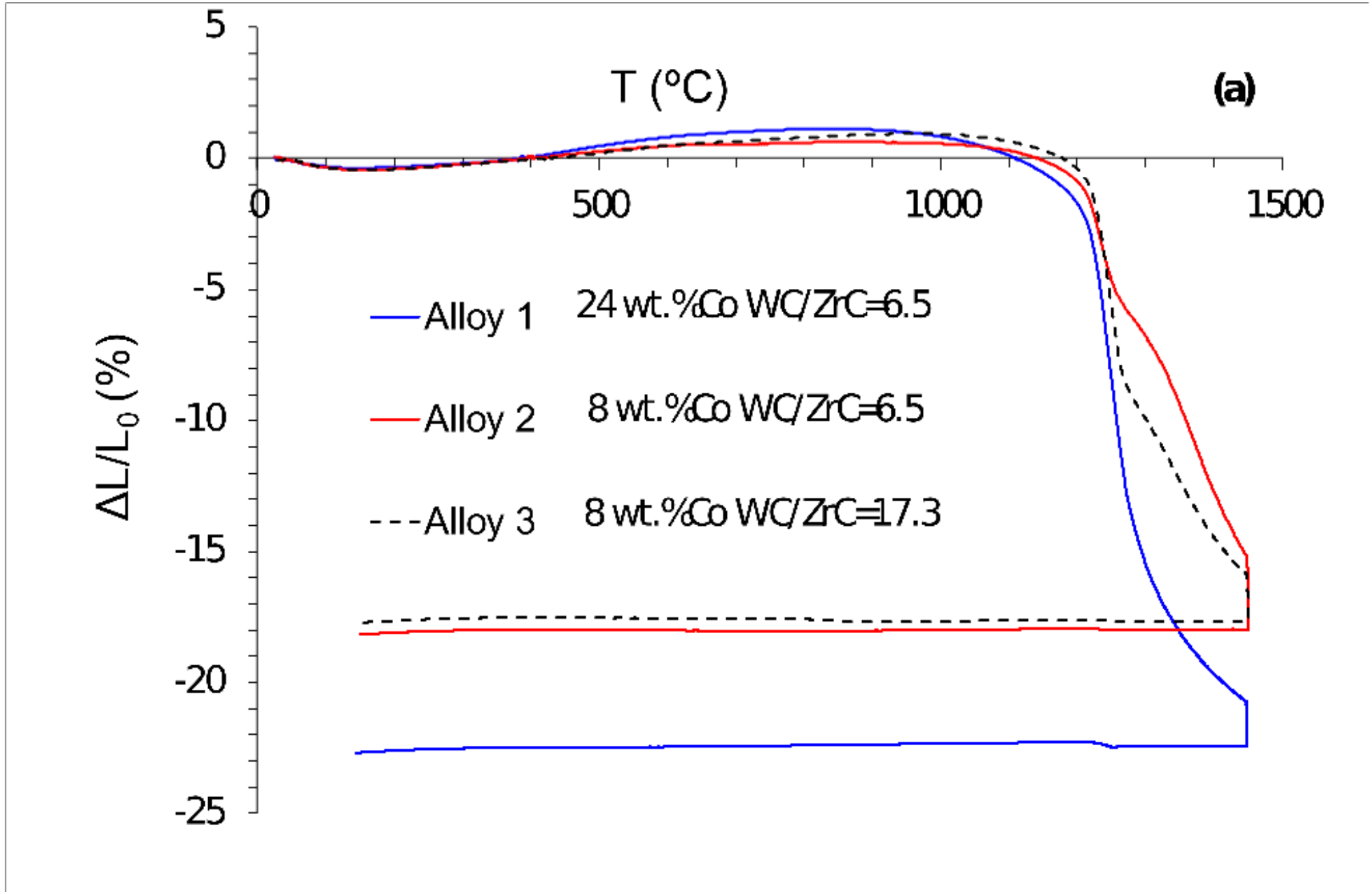
T (°C)
(a)
5
0
-5
-10
-15
-20
-25
0
500
1000
1500
ΔL/L0 (%)
Alloy 1 24 wt.%Co WC/ZrC=6.5
Alloy 2 8 wt.%Co WC/ZrC=6.5
Alloy 3 8 wt.%Co WC/ZrC=17.3

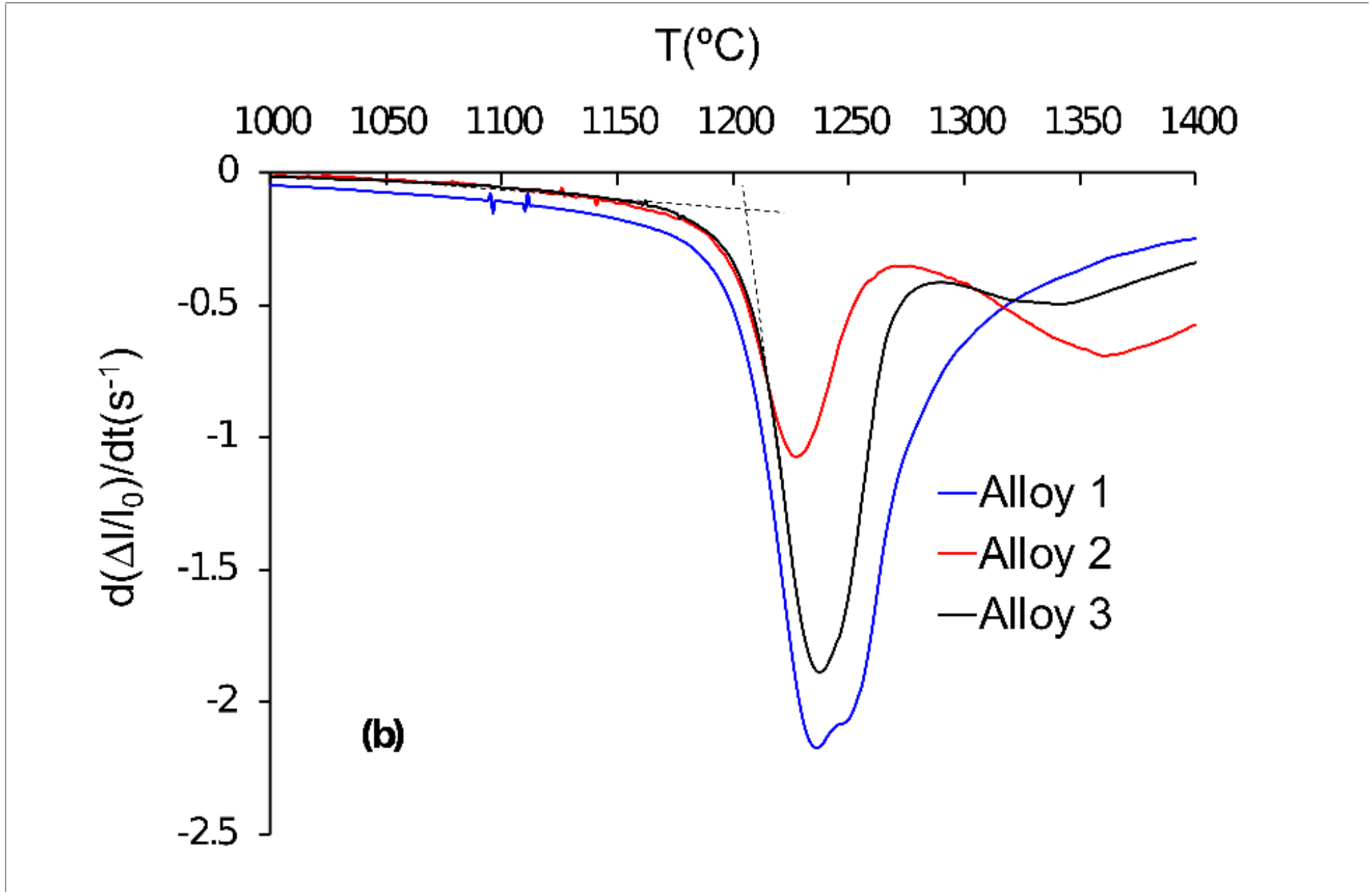
T(°C)
1000
1050
1100
1150
1200
1250
1300
1350
1400
0
-0.5
-1
-1.5
-2
-2.5
d(ΔI/I0)/dt(s-1)
(b)
Alloy 1
Alloy 2
Alloy 3

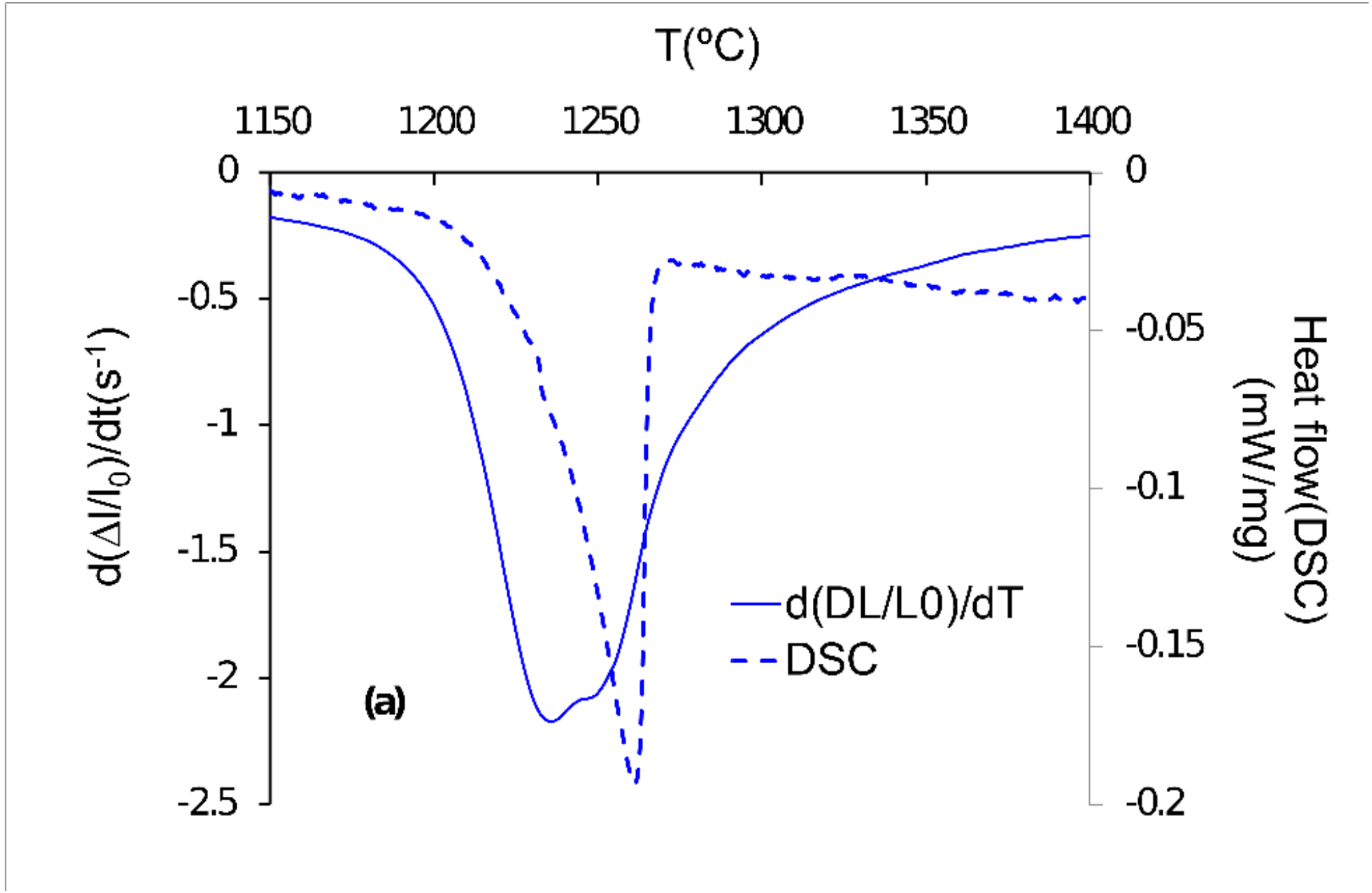
T(°C)
1150
1200
1250
1300
1350
1400
0
-0.5
-1
-1.5
-2
-2.5
d(ΔI/I0)/dt(s-1)
0
-0.05
-0.1
-0.15
-0.2
Heat flow(DSC) (mW/mg)
d(DL/L0)/dT
DSC
(a)

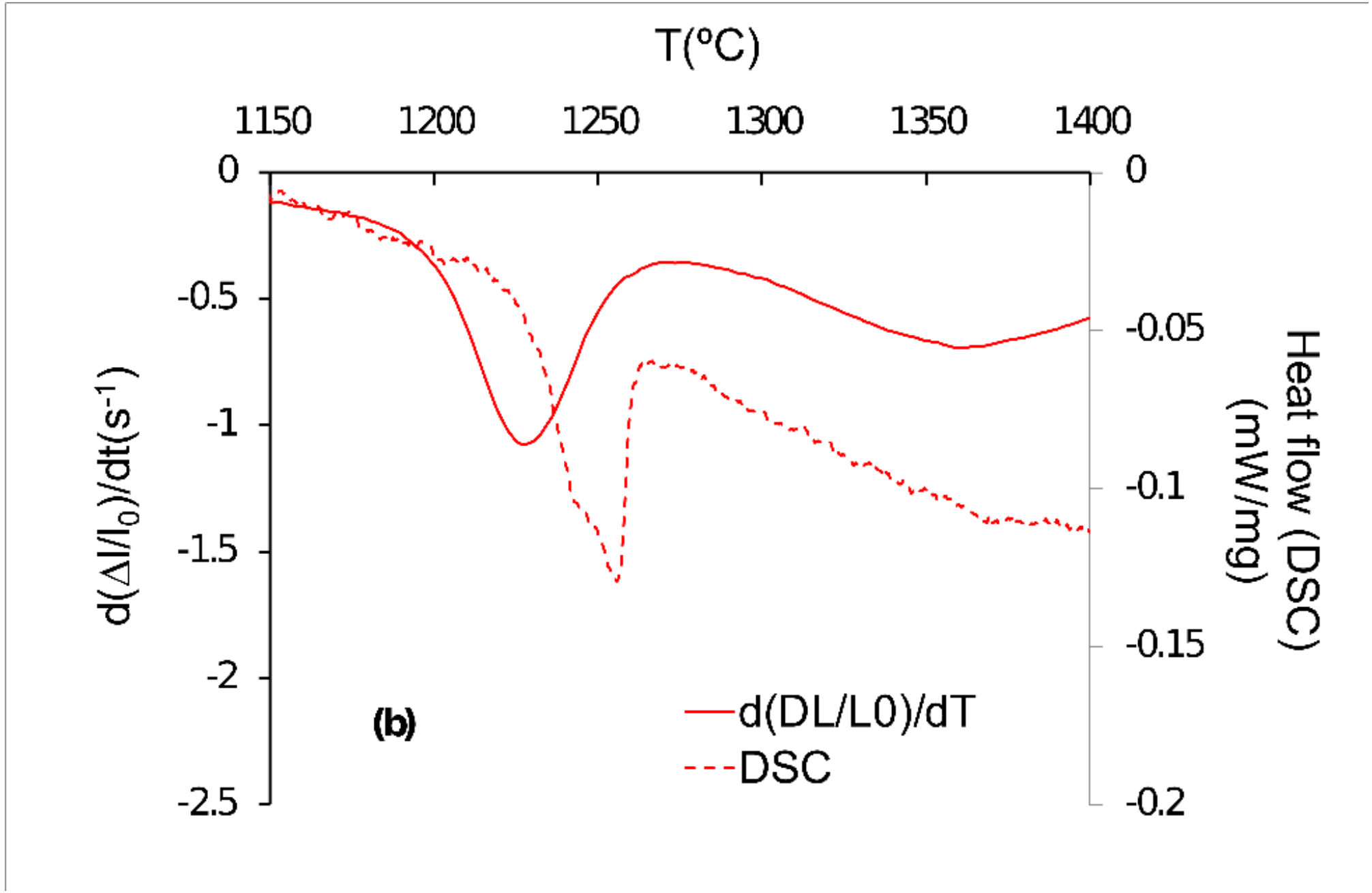
T(°C)
1150
1200
1250
1300
1350
1400
0
-0.5
-1
-1.5
-2
-2.5
0
-0.05
-0.1
-0.15
-0.2
d(ΔI/I0)/dt(s-1)
Heat flow (DSC) (mW/mg)
(b)
d(DL/L0)/dT
DSC

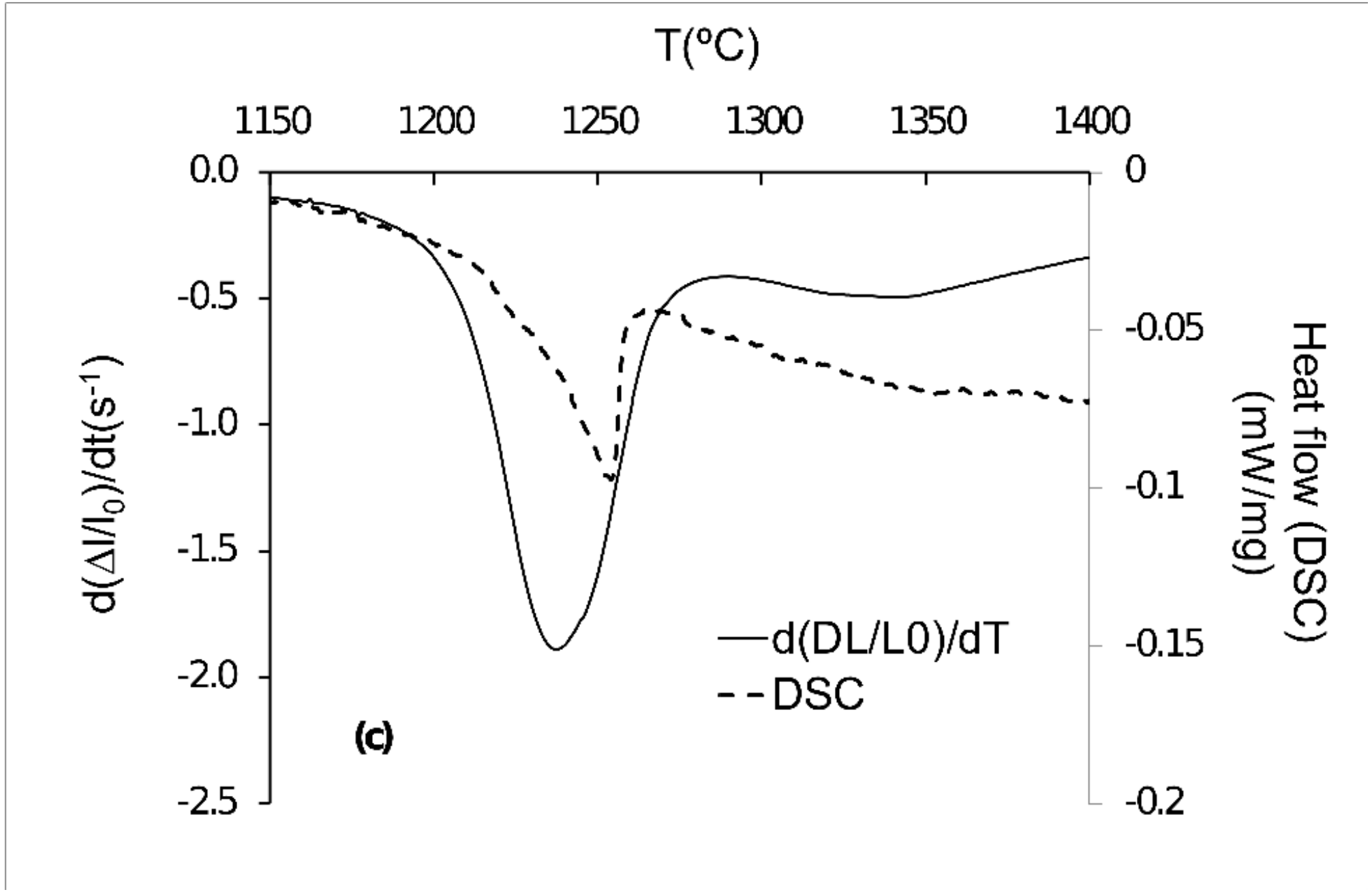
T(°C)
1150
1200
1250
1300
1350
1400
0.0
-0.5
-1.0
-1.5
-2.0
-2.5
0
-0.05
-0.1
-0.15
-0.2
d(ΔI/I0)/dt(s-1)
Heat flow (DSC) (mW/mg)
d(DL/L0)/dT
DSC
(c)

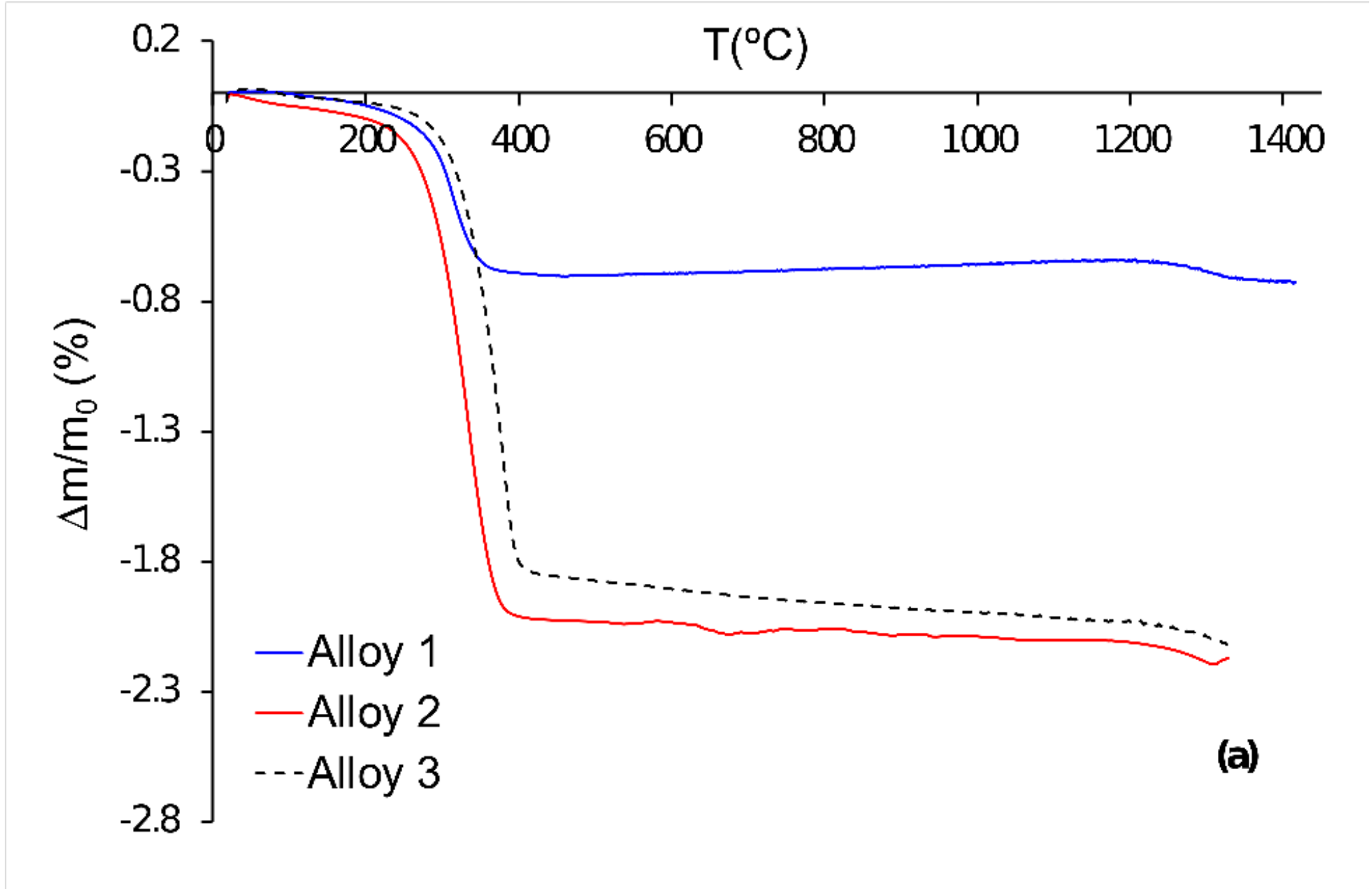
T(°C)
0.2
-0.3
-0.8
-1.3
-1.8
-2.3
-2.8
0
200
400
600
800
1000
1200
1400
Δm/m0 (%)
Alloy 1
Alloy 2
Alloy 3
(a)

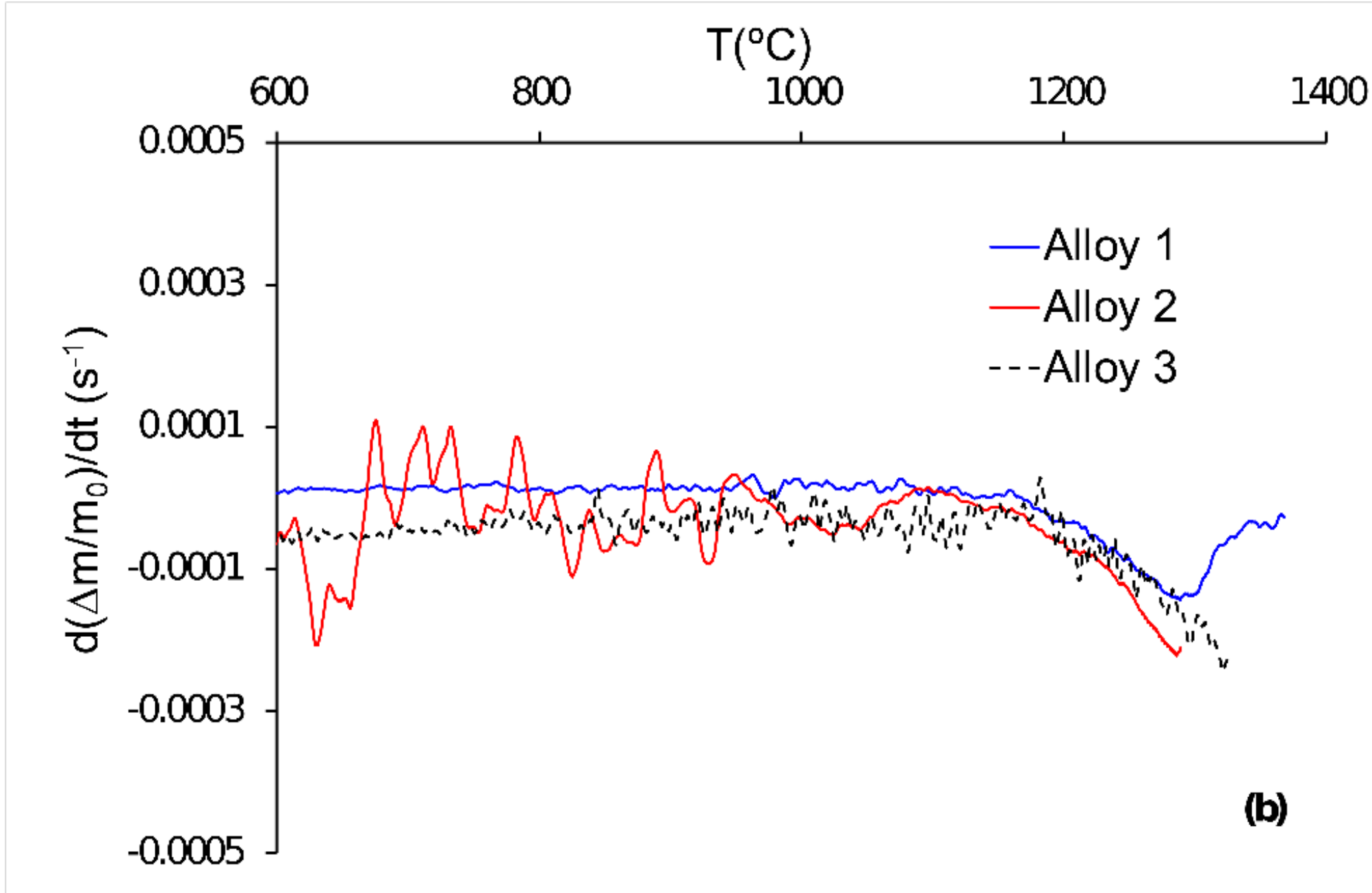
T(°C)
600
800
1000
1200
1400
0.0005
0.0003
0.0001
-0.0001
-0.0003
-0.0005
d(Δm/m0)/dt (s-1)
Alloy 1
Alloy 2
Alloy 3
(b)

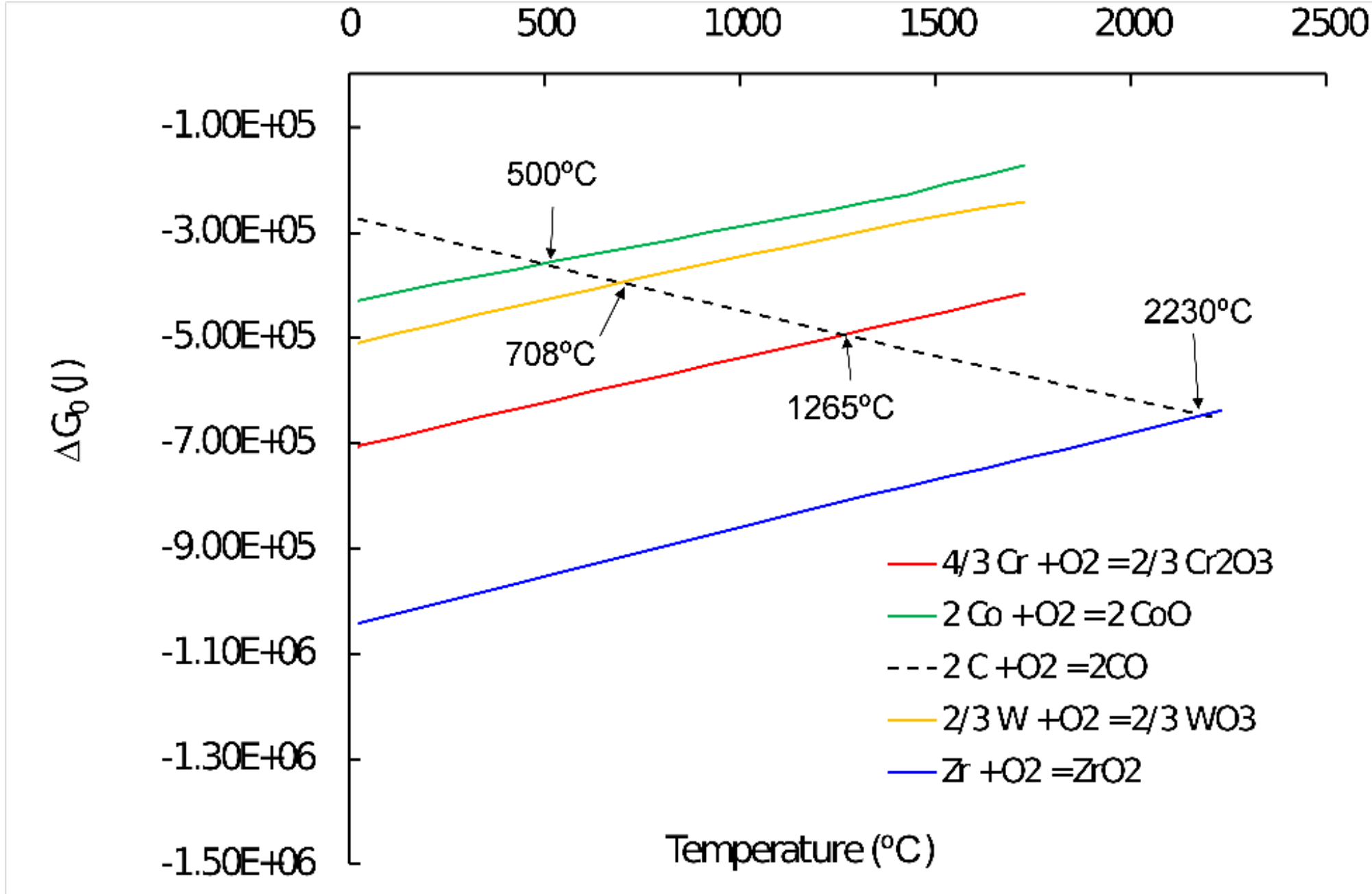
0
500
1000
1500
2000
2500
-1.00E+05
-3.00E+05
-5.00E+05
-7.00E+05
-9.00E+05
-1.10E+06
-1.30E+06
-1.50E+06
ΔG0 (J)
500°C
708°C
1265°C
2230°C
4/3 Cr +O2 =2/3 Cr2O3
2 Co +O2 =2 CoO
2 C +O2 =2CO
2/3 W +O2 =2/3 WO3
Zr +O2 =ZrO2
Temperature (°C)

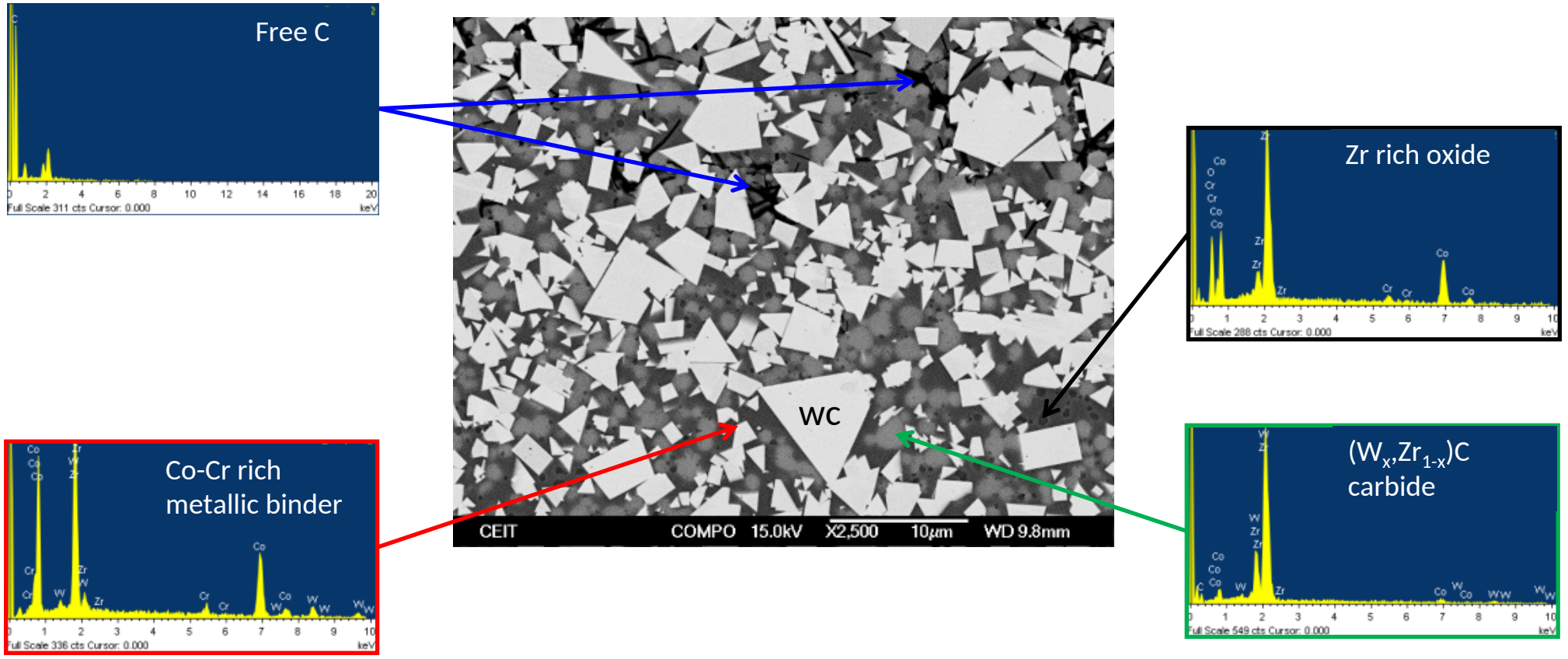
Free C
WC
Zr rich oxide
Co-Cr rich
metallic binder
(Wx,Zr1-x)C
carbide
CEIT COMPO 15.0kV X2,500 10μm WD 9.8mm

Fig. 5

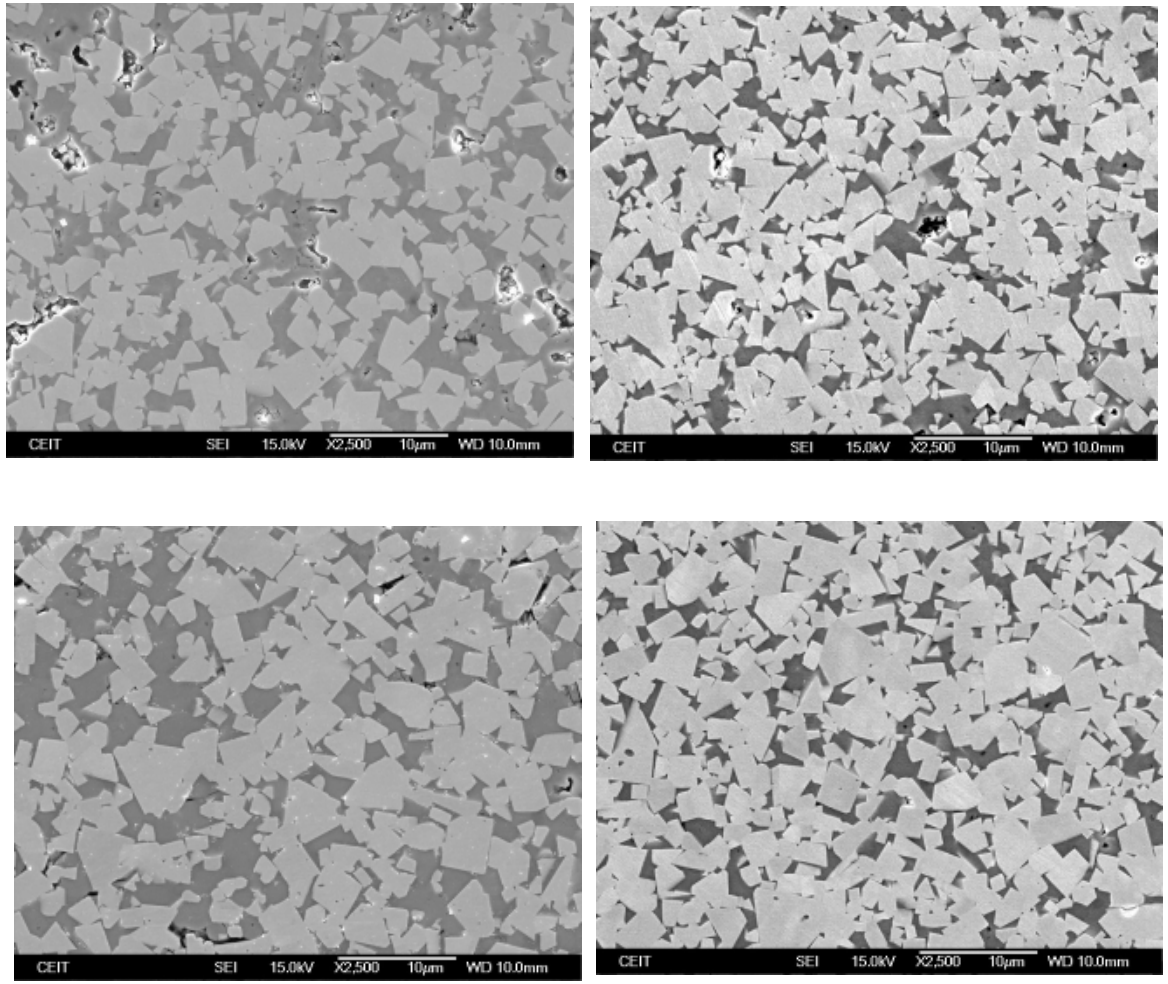
CEIT SEI 15.0kV X2,500 10μm WD 10.0mm
CEIT SEI 15.0kV X2,500 10μm WD 10.0mm
CEIT SEI 15.0kV X2,500 10μm WD 10.0mm
CEIT SEI 15.0kV X2,500 10μm WD 10.0mm

Fig. 6

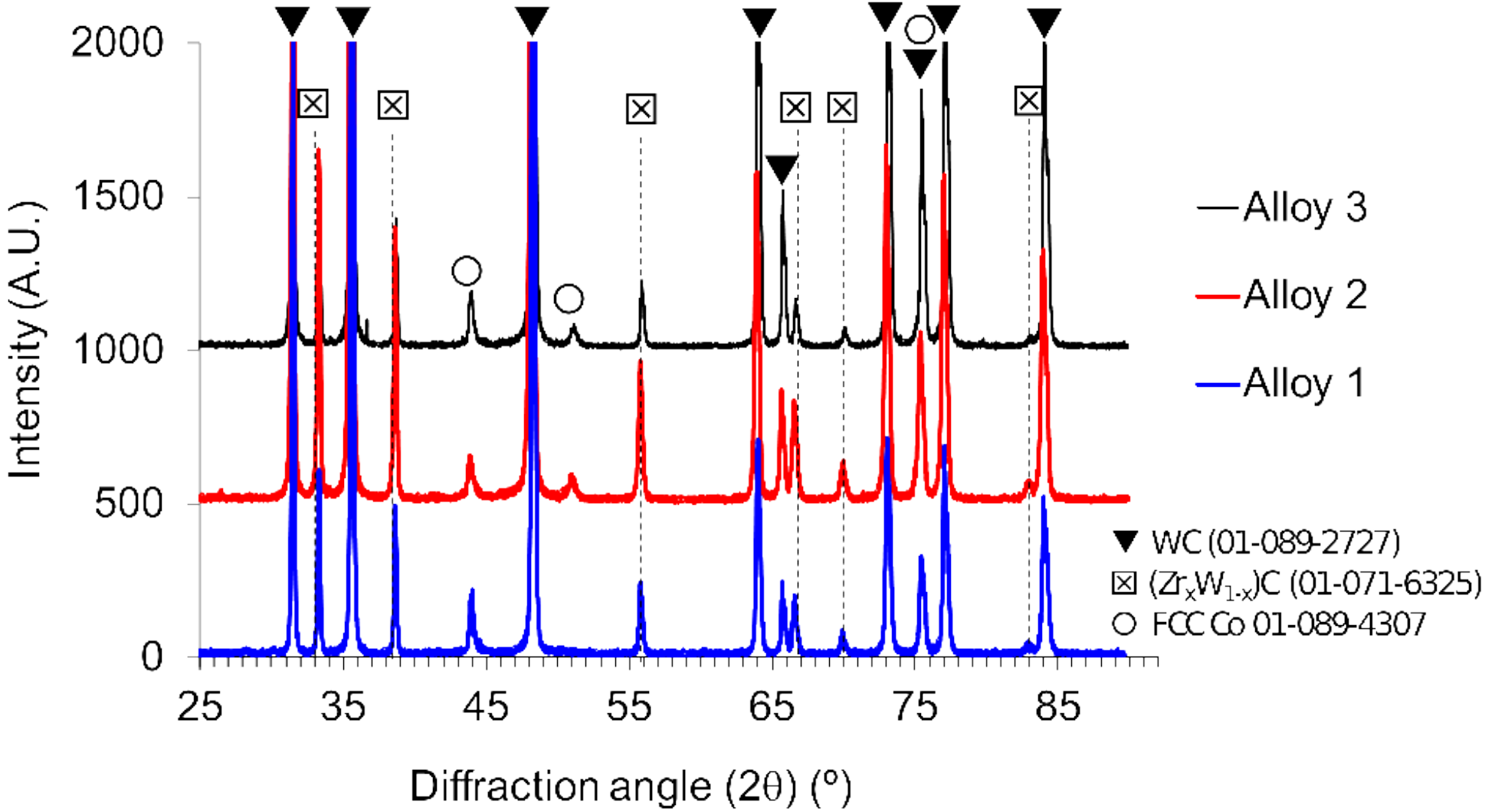
2000
1500
1000
500
0
Intensity (A.U.)
25
35
45
55
65
75
85
Diffraction angle (2θ) (°)
Alloy 3
Alloy 2
Alloy 1
WC (01-089-2727)
(ZrxW1-x)C (01-071-6325)
FCC Co 01-089-4307

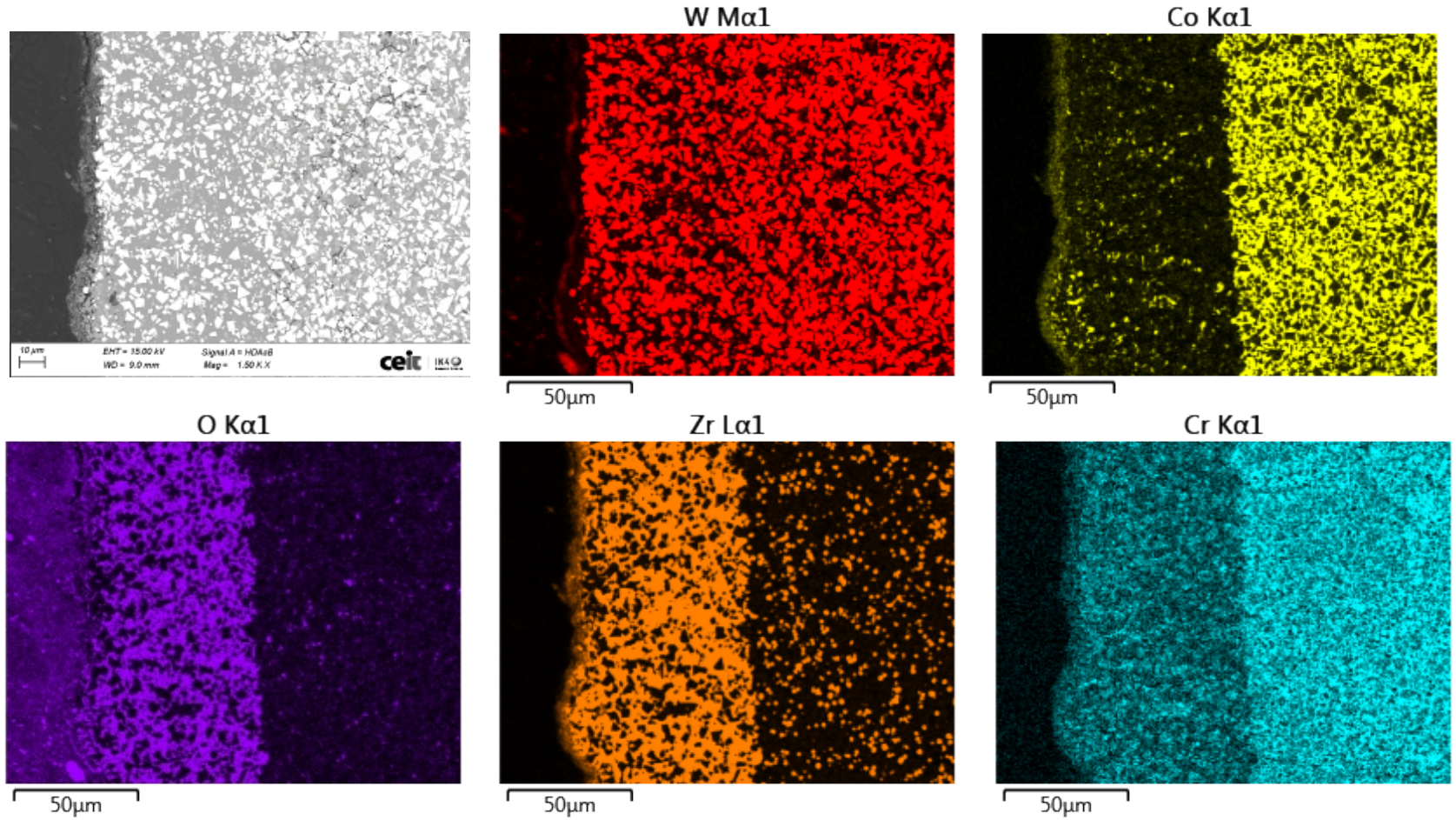

(a)

Fig. 8a

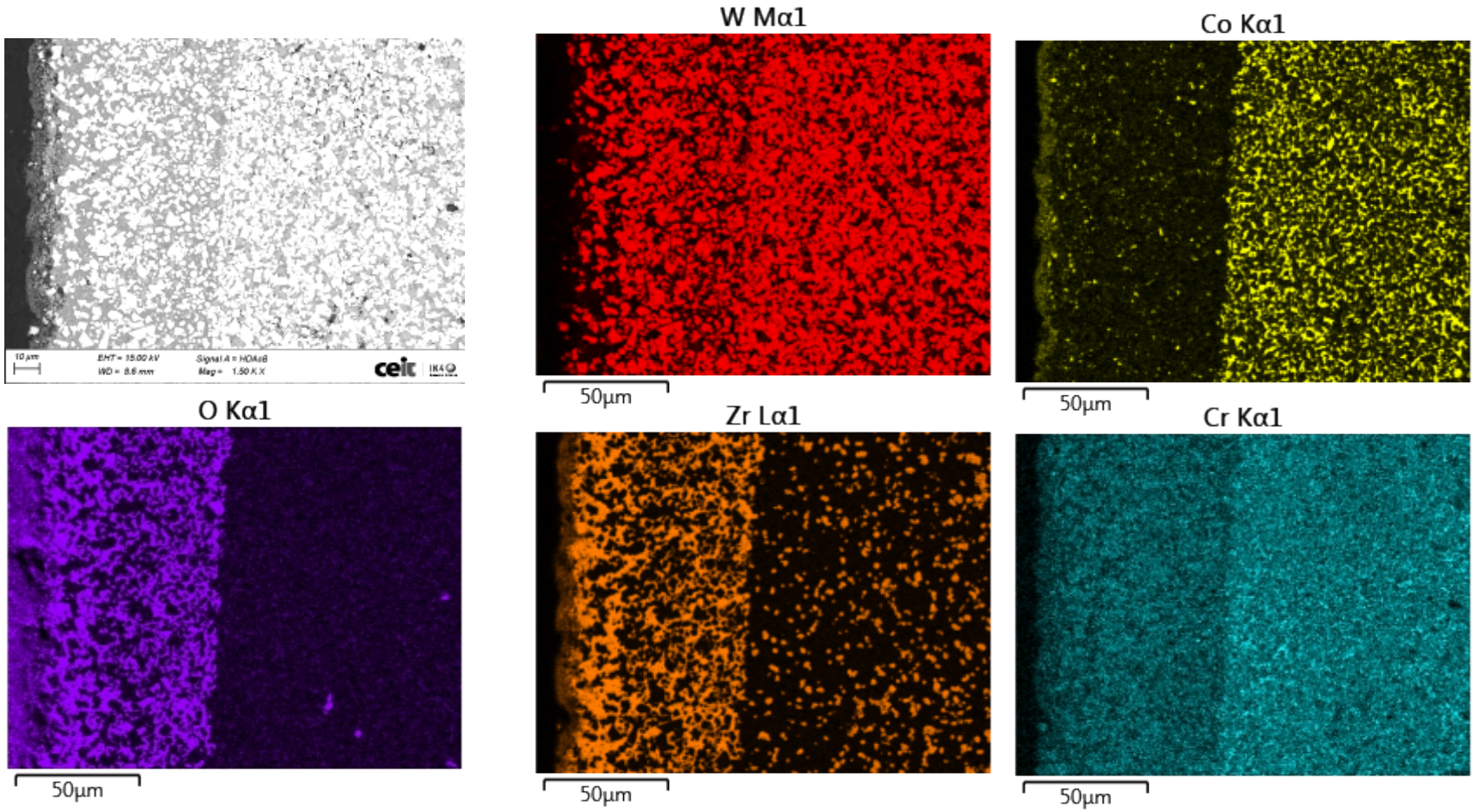

Fig. 8b

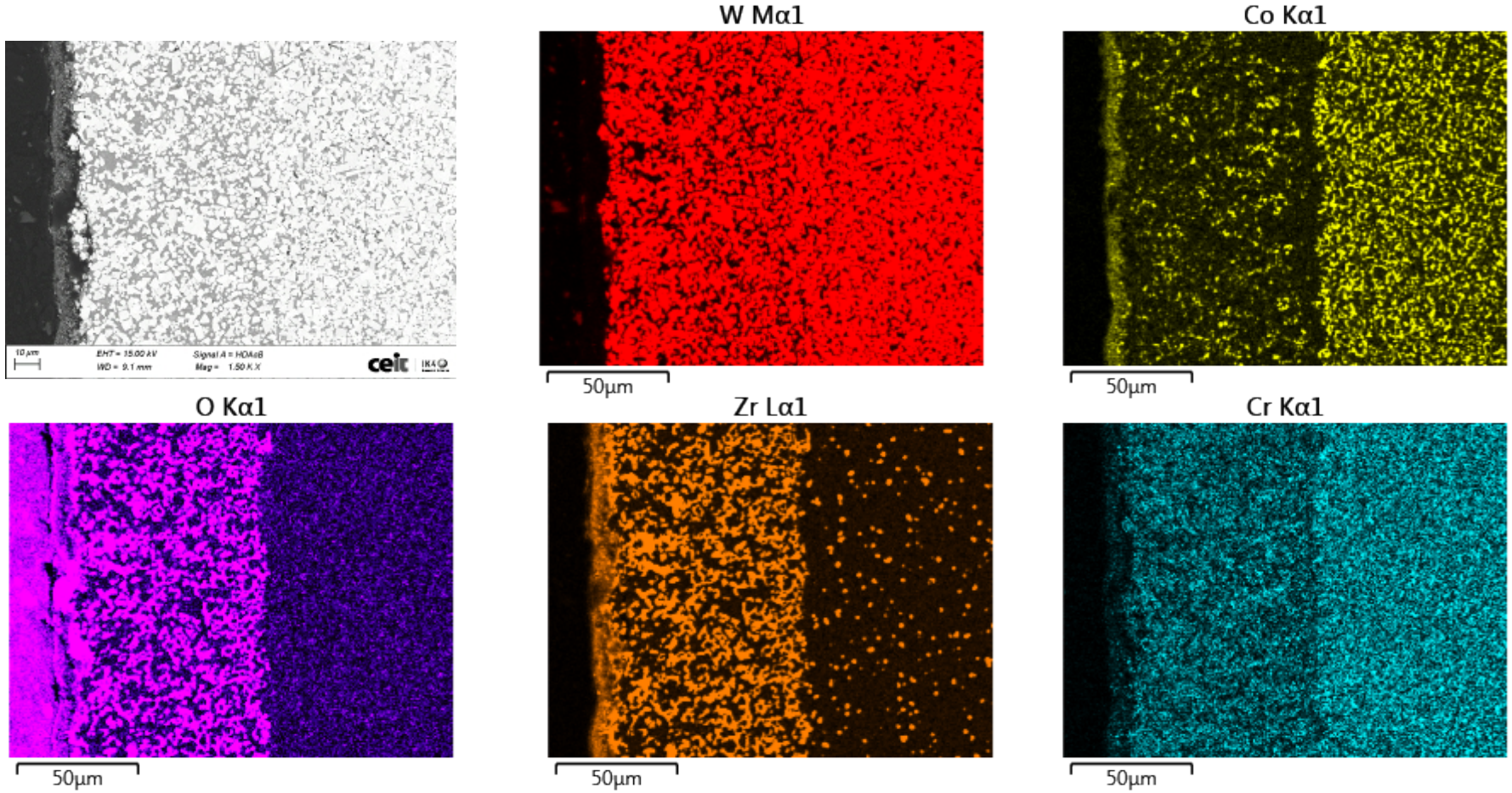

Fig. 8c

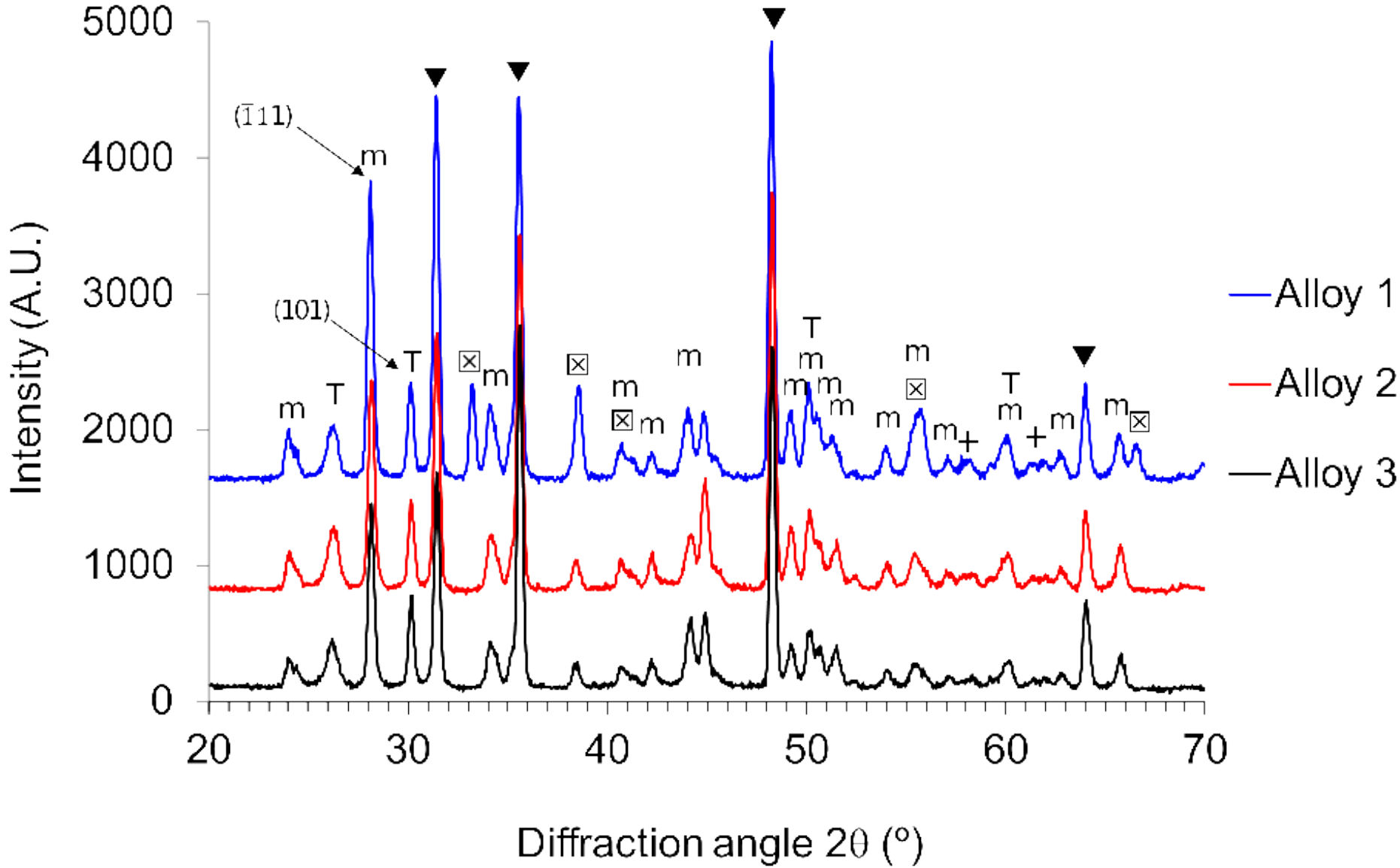
5000
4000
3000
2000
1000
0
Intensity (A.U.)
20
30
40
50
60
70
Diffraction angle 2θ (°)
(1̄11)
(101)
m
T
⊠
+
Alloy 1
Alloy 2
Alloy 3

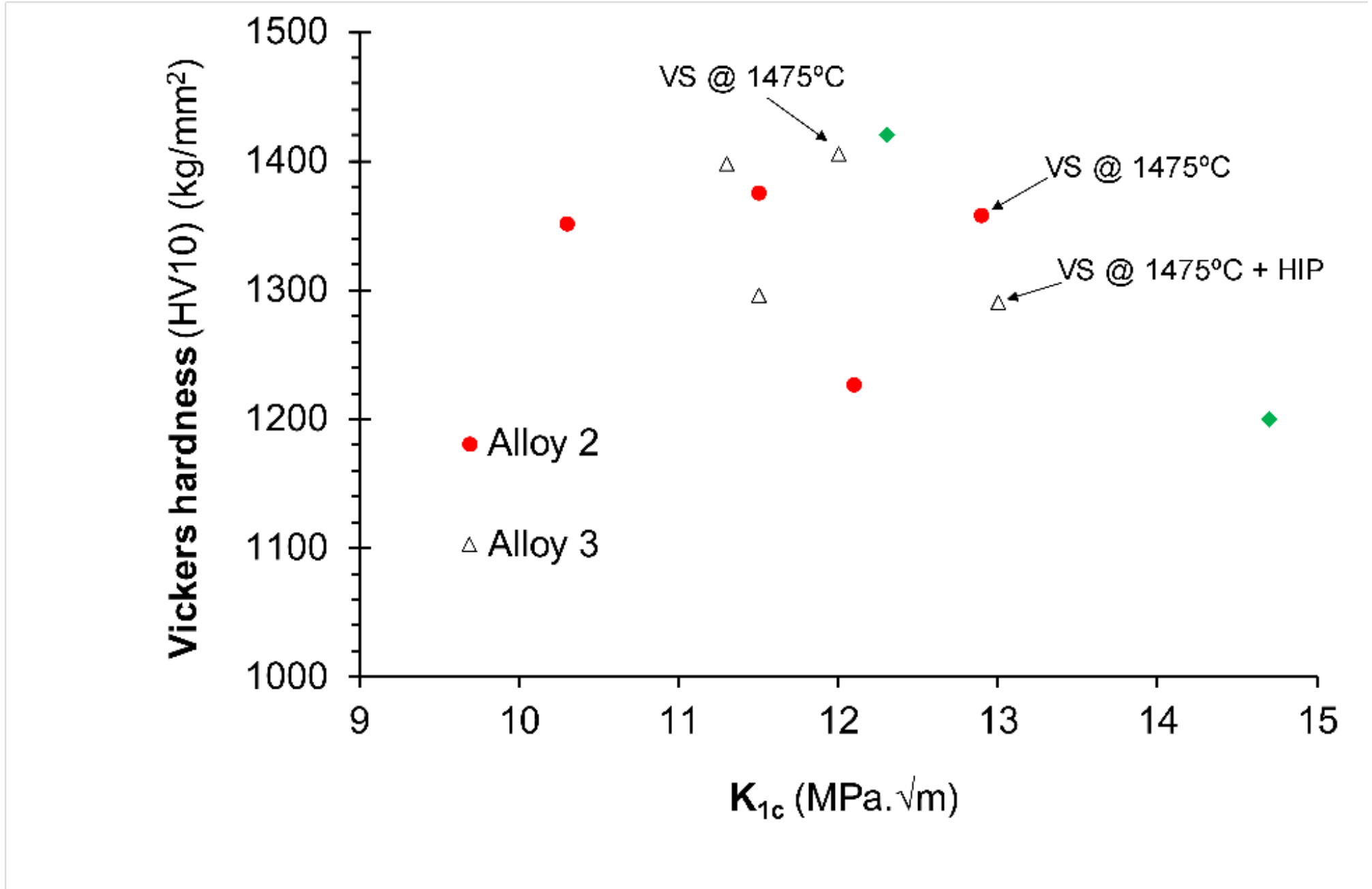
1500
1400
1300
1200
1100
1000
9
10
11
12
13
14
15
Vickers hardness (HV10) (kg/mm²)
K1c (MPa.√m)
VS @ 1475ºC
VS @ 1475ºC
VS @ 1475ºC + HIP
Alloy 2
Alloy 3

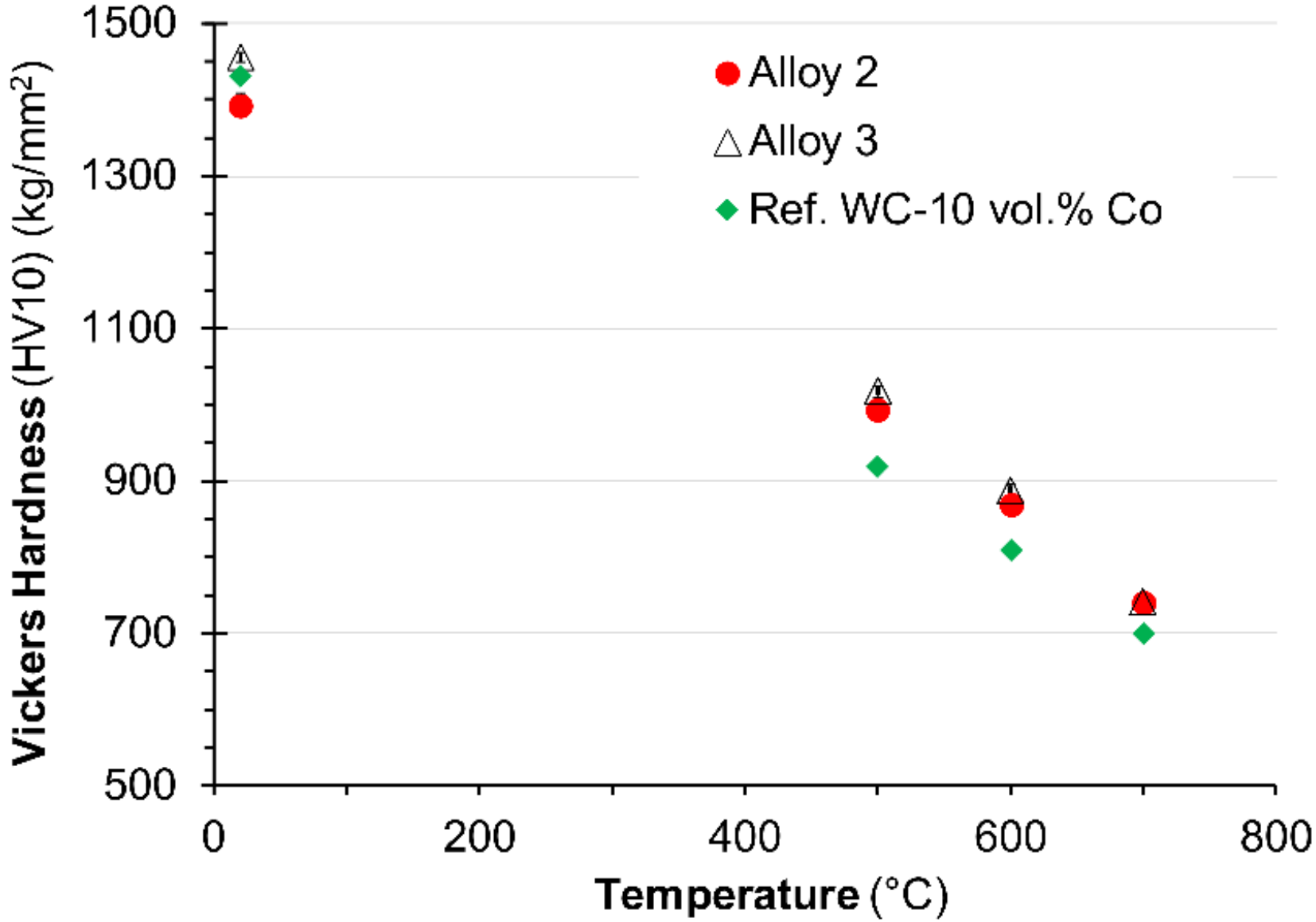
1500
1300
1100
900
700
500
Vickers Hardness (HV10) (kg/mm²)
Alloy 2
Alloy 3
Ref. WC-10 vol.% Co
0
200
400
600
800
Temperature (°C)

Table 1. Compositions of the powder mixtures (in wt.%)

Alloy	WC	Co	Cr_3C_2	ZrC	WC/ZrC Ratio (wt.%)	Theoretical density (g/cm^3)	Binder phase content (vol.%)
1	64.60	24.00	1.70	10.00	6.50	11.67	31.5
2	79.15	8.00	0.60	12.25	6.50	12.38	11.1
3	86.40	8.00	0.60	5.00	17.3	13.78	12.4

Table 2. Temperatures corresponding to shrinkage rate and DSC peaks

Alloy	Temperatures (ºC)				
	Shrinkage onset	**Maximum shrinkage**	**Melting onset**	**End of solidification**	**DSC peak**
1	1203	1235	1230	1180	1261
2	1200	1228	1229	1182	1255
3	1205	1238	1218	1180	1254

Table 3. Density corresponding to WC-ZrC-Co-Cr_3C_2 alloys obtained by vacuum sintering

	VS Temperature (ºC)					
	1400			1475		
	Porosity[1]	Density[2] (g/cm^3)	% T.D.	Porosity[1]	Density[2] (g/cm^3)	% T.D.
Alloy 1	A02/B00/C04	11,52	98.7	-	-	-
Alloy 2	A08/B04/C00	12,22	96.5	A06/B02/C00	12.44	98.3
Alloy 3	A06/B02/C00	13.27	96.2	A02/B00/C00	13.66	99.1
HIP after sintering[3]						
Alloy 2	A06/B04/C00	12.23	96.6	A02/B00/C00	12.51	98.8
Alloy 3	A06/B00/C00	13.48	97.8	A02/B00/C00	13.66	99.1

1- ISO 4499-4:2016

2- ISO 3369:2006

3- HIP parameters: 1400°C and 150 MPa for 1hour

Table 4. Carbon and oxygen contents of WC-ZrC-8 wt.%Co-Cr_3C_2 alloys processed by vacuum sintering (VS) and by HIP after VS (1400ºC-150MPa-1h)

	C content (wt.%)				**O content (wt.%)**		
	Theoretical*	Green compacts	After VS at 1400ºC-1h	After VS at 1475ºC-1h	Green compacts	After VS at 1400ºC-1h	After VS at 1475ºC-1h
Alloy 1	5.34	5.81±0.03	5.21±0.01	-	0.83±0.01	0.43±0.03	-
Alloy 2	6.35	7.84±0.03	6.39±0.03	6.52±0.06	0.50±0.03	0.11±0.01	0.11±0.02
Alloy 3	5.95	7.42±0.04	5.99±0.03	6.23±0.05	0.46±0.01	0.05±0.04	0.17±0.03
			After HIP + VS			After HIP + VS	
Alloy 2	6.35	7.84±0.03	6,42±0,01	6,50±0,04	0.50±0.03	0,22±0,03	0,23±0,06
Alloy 3	5.95	7.42±0.04	6,09±0,03	6,14±0,02	0.46±0.01	0,22±0,04	0,27±0,04

* Excluding the C content of the paraffin

Table 5. Lattice parameters corresponding to FCC metallic binder and $(Zr_x,W_{1-x})C$ phases of WC-ZrC-Co-Cr_3C_2 alloys processed by vacuum sintering (VS)

		Lattice parameter "a" (nm)					
		Alloy 1		**Alloy 2**		**Alloy 3**	
Phases	**Theoretical**	1400ºC	1475ºC	1400ºC	1475ºC	1400ºC	1475ºC
$(Zr_x, W_{1-x})C$	0,460(x=0.8)*	0,4658	-	0,4661	0,4650	0,4652	0,4648
Co	0,3544*	0,3561	-	0,3578	0,3574	0,3569	0,3572

* ICDD PDF-4 database

Table 6. EDS analyses corresponding to the surface oxide layers produced by the HIPing cycle in specimens previously sintered under vacuum at 1475ºC-1h

Composition (wt%)	**Alloy 1**	**Alloy 2**	**Alloy 3**
Zr	43	35	28
W	44	56	62
O	10	7	6
Co	3	2	3
Cr	<0.5	<0.5	<0.5

Table 7. Comparison of Vickers hardness (HV10) and WC mean grain size (WC G.S.*) of WC-ZrC-Co-Cr_3C_2 alloys processed by VS and VS+HIP.

	VS @ 1400ºC		**VS @ 1400ºC + HIP**		**VS @ 1475ºC**		**VS @ 1475ºC + HIP**	
	HV10 (kg/mm^2)	**WC G.S.** (µm)	**HV10** (kg/mm^2)	**WC G.S.** (µm)	**HV10** (kg/mm^2)	**WC G.S.** (µm)	**HV10** (kg/mm^2)	**WC G.S.** (µm)
Alloy 2	1227±16	1,7±0,2	1351±17	1,8±0,2	1358±15	1,9±0,2	1375±10	1,9±0,1
Alloy 3	1398±8	1,7±0,1	1296±12	1,9±0,2	1406±7	2,0±0,3	1291±24	2,1±0,2

* Measured by mean linear intercept method.

Declaration of interests

 The authors declare that they have no known competing financial interests or personal relationships that could have appeared to influence the work reported in this paper.

☐The authors declare the following financial interests/personal relationships which may be considered as potential competing interests:

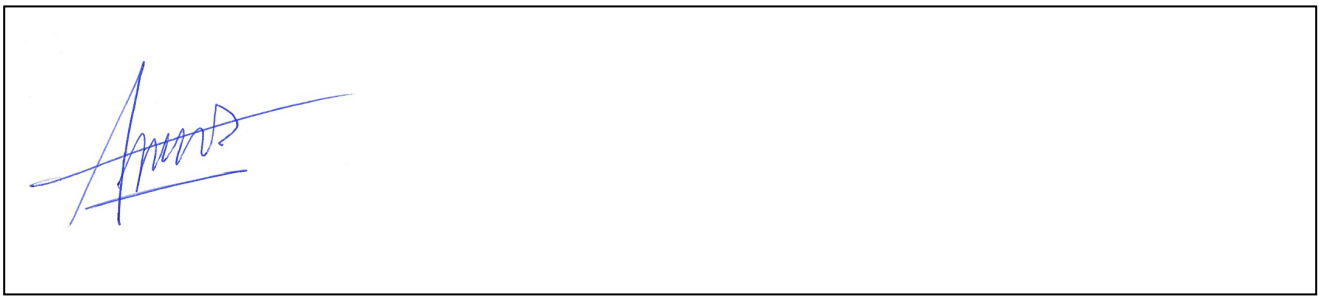

Tomas Soria: Investigation, Data curation, Writing- Original draft preparation.

Belen Lopez: Investigation, Data curation

Lorena Lozada: Investigation, Data curation, Writing- Original draft preparation.

Jose M. Sanchez: Conceptualization, Methodology, Writing-Review

Patricia Alveen: Validation, Project administration. Supervision, Funding acquisition

Steve Moseley: Validation, Project administration. Funding acquisition. Supervision

Ralph Useldinger Validation, Project administration. Supervision

Marc Elsen: Validation, Project administration. Supervision

M. Magin: Funding acquisition